

## **ABSTRACT**

MARROW, ETHAN ALEXANDER. Toward Hydrogel Microneedle Patches for the Passive Extraction of Subcutaneous Interstitial Fluid. (Under the direction of Michael A. Daniele).

The development of microneedles as intermediary devices between topical and hypodermic devices for body component analysis is described for biopolymer needles. The use of hyaluronic acid and hyaluronic acid-cellulose composites were used to develop microneedles with future applications in passively extracting interstitial fluid in a pain free manner. The described microneedles were fabricated through centrifugal force and facile EDC coupling. The resulting needles have demonstrated the ability to not only absorb fluid, but to continuously wick fluid across an impermeable membrane without the use of external pumps.

© Copyright 2017 Ethan Marrow

All Rights Reserved

Toward Hydrogel Microneedle Patches for The Passive Extraction of Subcutaneous  
Interstitial Fluid

by  
Ethan A. Marrow

A thesis submitted to the Graduate Faculty of  
North Carolina State University  
in partial fulfillment of the  
requirements for the degree of  
Master of Science

Biomedical Engineering

Raleigh, North Carolina

2017

APPROVED BY:

---

Dr. Michael A. Daniele  
Committee Chair

---

Dr. Ashley Brown

---

Dr. Zhen Gu

## DEDICATION

There are so many people and circumstances that have brought me to this point. First and foremost, I'd like to thank my mother, who has pushed me hard to succeed in whatever I chose. She has been a huge inspiration and has shaped me into the person I am today. I'd also thank the College of Charleston Department of Chemistry and Biochemistry and the faculty who taught me how to perform the elevated level critical thinking necessary for impactful scientific research. Holding your students to such a high standard has helped me immensely after graduation and has provided a high internal standard moving forward. Dr. Pat Woster, from the Medical University of South Carolina Department of Drug Discovery, who's mentorship I am reminded of every day. Truly a great chemist with a passion for pharmaceutical chemistry who has inspired me to pursue a career in clinical research. Finally, Dr. Daniele, who accepted me as his student despite my lack of familiarity his work and made this project possible. His passion for learning, regardless of topic, is highly admirable. His sense of duty to his students and position as a faculty member should be a benchmark to which all faculty are held.

I am deeply grateful for all the time and work these people have put into making me the best that I can be. I hope moving forward, I can not only meet their expectations, but also the lofty expectations I have set for myself because of encountering such amazing people.

Thank you all.

## **BIOGRAPHY**

Ethan Marrow was born on December 15, 1990 in Fredericksburg, Virginia. He grew up outside of Charleston, South Carolina and attended College of Charleston to pursue a bachelor's degree in Biochemistry. After graduating, Ethan worked at the Medical University of South Carolina as a chemist in Drug Discovery to gain a better understanding of the drug development process. He later moved to Raleigh, North Carolina to attend North Carolina State University's Biomedical Engineering program. Ethan completed his Master's degree in Biomedical Engineering in 2017.

## **ACKNOWLEDGMENTS**

I would like to thank Dr. Daniele and the BioInterface Laboratory for taking me on as a graduate student. Helping start a new lab and working with brand new faculty is always a privilege and an honor and Dr. Daniele is no exception. His passion for biomedical engineering and his constant pursuit of knowledge is truly inspirational. Despite his young age and career, he has proven to be an effective leader and mentor. Working with the BioInterface Laboratory has been very rewarding and has been a great experience!

## TABLE OF CONTENTS

<b>LIST OF TABLES</b> _____	viii
<b>LIST OF FIGURES</b> _____	ix
<b>INTRODUCTION</b> _____	1
SIGNIFICANCE OF INTERSTITIAL FLUID _____	2
CURRENT METHODS IN INTERSTITIAL FLUID COLLECTION _____	6
IONTOPHORESIS _____	6
SONOPHORESIS _____	8
SUCTION BLISTER METHOD _____	11
WICK-IN-NEEDLE METHOD _____	14
MECHANICAL PUMPS _____	15
CURRENT MICRONEEDLE TECHNOLOGY _____	19
MICRONEEDLE HISTORY _____	20
MICRONEEDLE DESIGN AND APPLICATIONS _____	22
<b>SIGNIFICANCE OF PROJECT (OVERVIEW)</b> _____	33
DETAILED SYNOPSIS _____	35
MATERIALS OF INTEREST _____	35
SPECIFIC TESTING GOALS _____	38
<b>MATERIALS &amp; METHODS</b> _____	40
MATERIALS _____	40
METHODS _____	41
SOLUTION PREPARATION _____	41
MICRONEEDLE FABRICATION _____	41
FILM ABSORPTION _____	42
MICRONEEDLE SWELLING _____	43
FLUID WICKING _____	43
MECHANICAL CHARACTERIZATION _____	45
DERMAL PUNCTURE TESTING _____	46
<b>RESULTS &amp; DISCUSSION</b> _____	47
FILM ABSORPTION _____	47
MICRONEEDLE FABRICATION _____	49
MICRONEEDLE SWELLING _____	51
MICRONEEDLE WICKING _____	53
MICRONEEDLE COMPRESSION _____	54

DERMAL PUNCTURE TEST _____	57
<b>CONCLUSIONS &amp; FUTURE DIRECTION</b> _____	58
<b>REFERENCES</b> _____	60
<b>APPENDIX A</b> _____	77
CELLULOSE CULTURE PROTOCOL _____	79
MECHANICAL TESTING METHODS _____	82
RESULTS & DISCUSSION _____	83

## LIST OF TABLES

<b>Table</b>	<b>Page Number</b>
Table 1. Equations for microneedle mechanics _____	41
Table 2. Full width half max data _____	55

## LIST OF FIGURES

<b>Figure</b>	<b>Page Number</b>
Figure 1. Importance of continuous monitoring _____	2
Figure 2. Negative pressure of ISF _____	4
Figure 3. Illustration of the epidermis _____	5
Figure 4. Electrophoresis schematic _____	6
Figure 5. Reverse electrophoresis schematic _____	7
Figure 6. Sonophoresis schematic _____	9
Figure 7. Sonic cavitation schematic _____	10
Figure 8. Suction blister schematic _____	11
Figure 9. Suction blister array and excision _____	13
Figure 10. Needle wick extraction diagram _____	14
Figure 11. Microdialysis diagram _____	16
Figure 12. Open-flow microperfusion diagram _____	17
Figure 13. Modes of microneedle application _____	24
Figure 14. Solid coated microneedle examples _____	25
Figure 15. Example of microneedle materials _____	27
Figure 16. Examples of hollow-bore microneedles _____	28
Figure 17. Examples of dissolving microneedles _____	30
Figure 18. Swelling of hydrogel microneedle _____	31
Figure 19. Projection of hyaluronic acid _____	37
Figure 20. EDC crosslinking mechanism _____	38
Figure 21. Schematic of microneedle formation _____	44
Figure 22. Full-width half-max swelling image _____	46
Figure 23. Paper pump microneedle schematic _____	47
Figure 24. Microneedle compression setup _____	48
Figure 25. Thin film absorption bar graph (2% vs 4% solids) _____	50
Figure 26. Thin film absorption bar graph (HA vs Composite) _____	48
Figure 27. SEM image of HA microneedles _____	50
Figure 28. Microneedle array full view _____	51
Figure 29. SEM of HA microneedle with high magnification _____	53
Figure 30. SEM of Cellulose microneedle with high magnification _____	55
Figure 31. Full width half max microneedle swelling data _____	56

Figure 32. Microneedle fluid transport on paper pump _____	58
Figure 33. Mechanical compression of HA microneedles (effect of length) _____	59
Figure 34. Mechanical compression of microneedles (HA vs. Composites) _____	60
Figure A1. Microbial cellulose culture dish _____	A3
Figure A2. Mechanical tests of wet cellulose composite _____	A6
Figure A3. Mechanical tests of dry cellulose composite _____	A7

## Introduction

With the growing desire to achieve a “quantified self,” continuous monitoring of every aspect of daily life has become a big business. The quantified self is the notion that monitoring personal physiological data, such as heart rate, pulse, calorie consumption, etc. can lead to more healthy lifestyles.<sup>13</sup> Companies such as Apple, FitBit, Garmin, and more have all begun capitalizing on the fitness tracking craze, but their initial investment in health monitoring and maintenance has given rise to interest in continuous health monitoring of disease states and clinical health monitoring.

Current methods in clinically relevant health monitoring rely on periodic measurements taken in a clinical setting or using clinical devices on their own. This entails the patient be trained to either travel to a clinician to undergo testing or be trained to test themselves. Testing of analytes and metabolites often requires a blood sample, which means pain and puncturing of the protective outer layer of the skin. The inconvenience and risks associated with blood-based monitoring methods result in trepidation and reduced compliance on the patient’s part. To further exacerbate the problem, the nature of periodic monitoring is insufficient to accurately measure the clear majority of a specific analyte concentration over the course of a day.

**Figure 1** exemplifies the importance of continuous monitoring. In the example, if a patient required monitoring at every fifth time point, it would appear that the analyte concentration is only within the desired range about 43% of the time, under 43% of the time, and over by 14% of the time. A continuous monitoring of the same data would show the patient is actually within the desired range around 53% of the time, over by 24% of the time, and under

### Example of Bolus Delivery Concentration Model

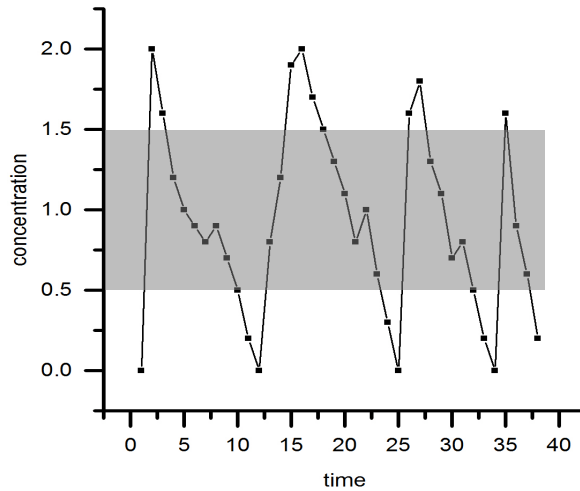


**Figure 1:** Example chart demonstrating the utility of continuous monitoring system. Points represent periodic concentrations while the grey section represents an exemplary therapeutic range.

by 21% of the time. The two interpretations of this sample data in the clinical setting could really affect diagnoses and medication regimens and could also mean the difference between life and death for some patients.

Continuous monitoring of metabolites and analytes could lead to better understanding of diseases and could provide helpful data to physicians trying to treat their patients in an effective manner.<sup>14-22</sup> Wearing a continuous access port, such as a hypodermic needle, would put patients at a severe risk for infection or vascular damage.<sup>23</sup> Nonetheless, a continuous monitoring system will be required for furthering the knowledge of disease states, metabolism, and general health of an individual and a population.

### *Interstitial Fluid*

Interstitial fluid is the fluid that exists between the cells within an animal's body. Interstitial fluid (ISF) is formed as blood plasma permeates out of the blood vessels. As the plasma permeates into the surrounding tissue, it brings with it many of the plasma components (small molecules, ions, and hormones), while leaving behind plasma proteins, red blood cells, and platelets.<sup>24-27</sup> Furthermore, ISF is the media through which cellular waste is removed. This characteristic could give better insight to metabolic processes and abnormalities therein. As the ISF carries many of the same components of plasma as well as other important biomarkers, it has become a target for pain-free health analysis while avoiding direct contact with the cardiovascular system and still providing valuable health data.

When using the ISF as a media for analysis, several important factors must be taken into consideration concerning the physical and chemical differences between the ISF and blood. As mentioned previously, ISF carries many of the same analytes found in plasma with one significant difference: ISF concentrations of many analytes are much lower than in plasma, often by one to two orders of magnitude. This discrepancy could be a hurdle to the development of metabolite analyzing devices in the future since many "physiological concentrations" of analytes are often only known for blood plasma. ISF is also a unique bio-fluid with respect to its physiological pressure.

Most fluids within the body hold a positive or neutral pressure relative to the atmosphere. ISF is unique in that its pressure is usually positive throughout the body, but becomes negative at the atmospheric interfaces at the skin and lungs.<sup>3</sup> This ensures that our outer layer of skin (epidermis) remains bonded to the dermis and also ensures that interstitial fluid does not permeate out through the epidermis and stratum corneum. Although

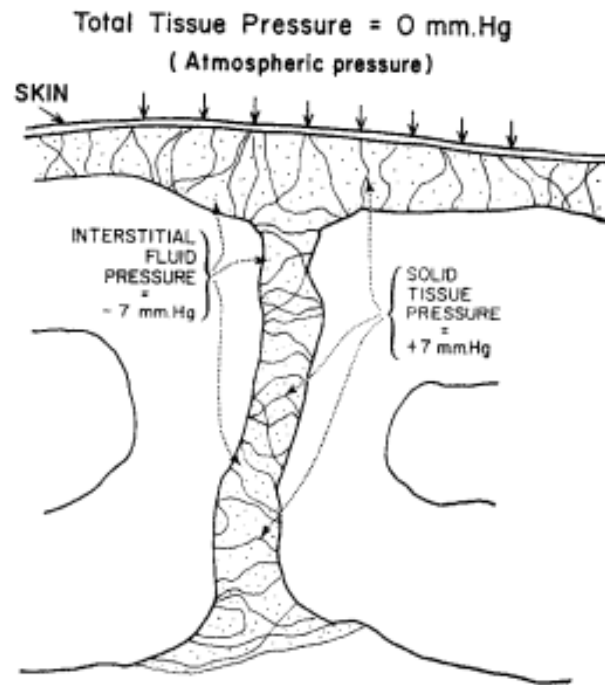


**Figure 2:** Effect of negative interstitial fluid pressure on other types of tissue pressure.<sup>3</sup> Reprinted with permission from the American Physiological Society.

physiologically vital, the negative subcutaneous interstitial fluid pressure creates a hurdle for extraction.

ISF has been a target for medical analysis due to its ability to provide relevant metabolite data. There are several historical methods used for the extraction and analysis of ISF, but blood plasma remains the gold standard for diagnostics. The reliance on blood plasma is largely because blood plasma generally has more concentrated analytes<sup>28-34</sup> than does interstitial fluid and is already a free-flowing fluid.

Facile acquisition of ISF could lead to improved quality of life for a large percentage of the population by replacing unnecessary needle sticks. Furthermore, use of microneedle

patches for delivery and analysis techniques would reduce the risk of accidental needle-stick contamination by hospital staff. The reduction of needle use in both home and clinical settings could dramatically reduce the burden placed on the healthcare system by accidental disease transmission, as well as the cost associated with infection treatment.

Challenges to ISF collection are numerous.<sup>35-38</sup> Extraction of ISF has been relatively challenging compared to blood. Currently, all that is required for a blood sample is a needle and collection vessel.<sup>39-43</sup> ISF is created by plasma transfer across vascular walls. Because ISF exists as a filler fluid, ISF has no direct route for access like blood and attempts to access ISF

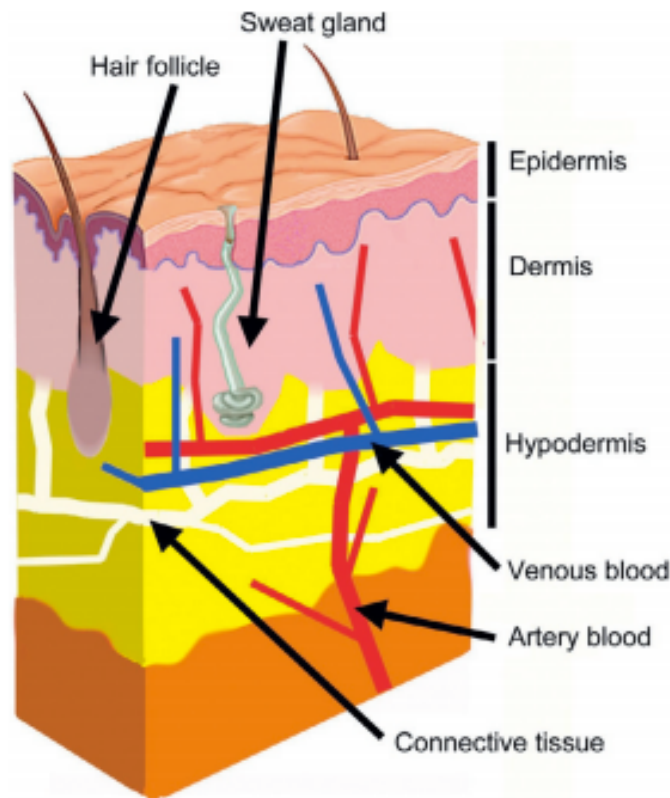


**Figure 3:** Structure of skin. Note that blood does not flow into the epidermis. Reproduced with permission from Elsevier.<sup>1</sup>

without blood contamination is a tricky process.<sup>44-48</sup> In attempts to overcome this obstacle, scientists have utilized a variety of techniques to get at the fluid including: ion gradient formation, blister formation, insertion of pumps, placing wicks in the skin, and more.

While this section highlights the utility of each of the methods of ISF extraction, none are completely effective for the task of continuously extracting ISF for health monitoring. The following methods have primarily been developed as drug delivery tools. They have all shown flexibility of application though and have demonstrated some efficacy in their abilities to extract ISF. While none perform at the level required for continuous, pain-free monitoring, the past work is the foundation for all future work in ISF extraction and without which, the current state of the art would not be advancing as it is.

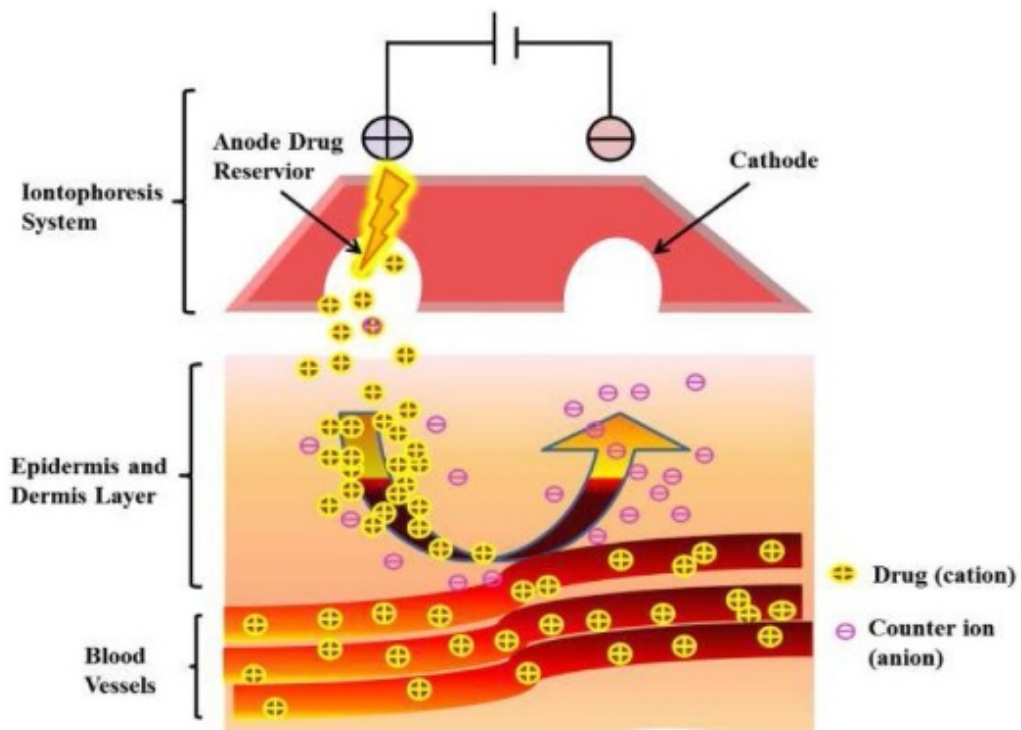


**Figure 4:** Schematic of iontophoresis used for drug delivery.

Iontophoresis is a process by which electrical current drives ions through a medium using electro-osmosis. This method has been a heavy source of investigation for more than 100 years.<sup>49</sup> The early pioneers of iontophoresis found medical significance for the technique as a means to get ionic molecules into the skin. Due to the limited range of study drugs at the time, many studied iontophoresis using acetyl-beta-methylcholine as it is a charged amine that would not otherwise cross the SC.<sup>50</sup>

Before the advent of ethics committees, iontophoresis was also used to deliver bleaching agents to the cornea<sup>51</sup> and test the pain thresholds of humans.<sup>52</sup> Historically, iontophoresis has been used to transdermally deliver a variety of compounds<sup>50,53-58</sup> but delivery is limited to either charged or polar molecules of low molecular weight.

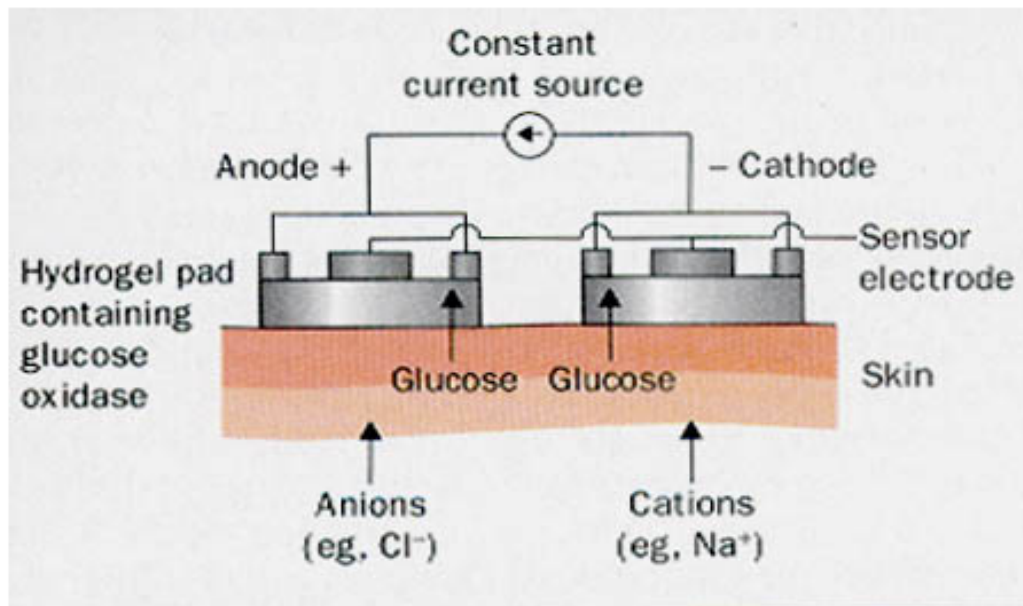


**Figure 5:** Reverse iontophoresis as described in the GlucoWatch patent.<sup>2</sup>

Over the course of iontophoresis research, many new drugs with polar and/or charged regions entered the market. The development of these drugs enabled greater iontophoresis

research for a wide range of applications. Classical-type drugs, such as terbinafine (antifungal),<sup>59</sup> sumatriptan (antimigraine),<sup>60</sup> and more<sup>58</sup> have been delivered as expected, but recent work has demonstrated the ability of iontophoresis for delivery of large molecules across the stratum corneum.<sup>61</sup> The ability to deliver large molecules has been utilized with proteins,<sup>62</sup> polysaccharides,<sup>63</sup> nucleic acid chains,<sup>64</sup> and nanoparticles.<sup>65</sup>

While typical iontophoresis uses repulsive fields to drive drugs same-charged molecules into the bloodstream across the stratum corneum, reverse iontophoresis is a process used to pull ions towards an oppositely charged electrode. Reverse iontophoresis is used for sampling ISF analytes without penetrating the SC. This technology has been used to sample many types of analytes.<sup>26,34,66-71</sup> Lithium ions have been used to treat mental health disorders for a long time. Iontophoresis has been used as a method to draw lithium ions from the subcutaneous ISF.<sup>72</sup> By far the greatest push for iontophoresis-driven extraction of analytes has been geared towards glucose monitoring in diabetes, which has resulted in the patent and production of the GlucoWatch<sup>73</sup> by Cygnus, which has since been discontinued due to high cost, poor performance, and low customer satisfaction.

Despite the potential advantages of iontophoresis, there have been some obvious limitations. It has been demonstrated that the ability for iontophoresis to deliver therapeutics into deep tissue in a targeted fashion is not as effective as surgical options.<sup>74</sup> Electrophoresis is also a poor choice for large molecule delivery without preparation via microporation of the SC.<sup>62,75</sup> While aspects of iontophoresis may not be suitable for all applications of drug delivery and ISF sampling, it has been shown to be effective at extracting a wide variety of analytes,

but due to the negatively charged surface of the skin, anionic molecules remain poor targets for analysis.<sup>76</sup>

One less commonly known form of transmembrane access uses high frequency sound waves to introduce or extract fluids across the stratum corneum. This method is called

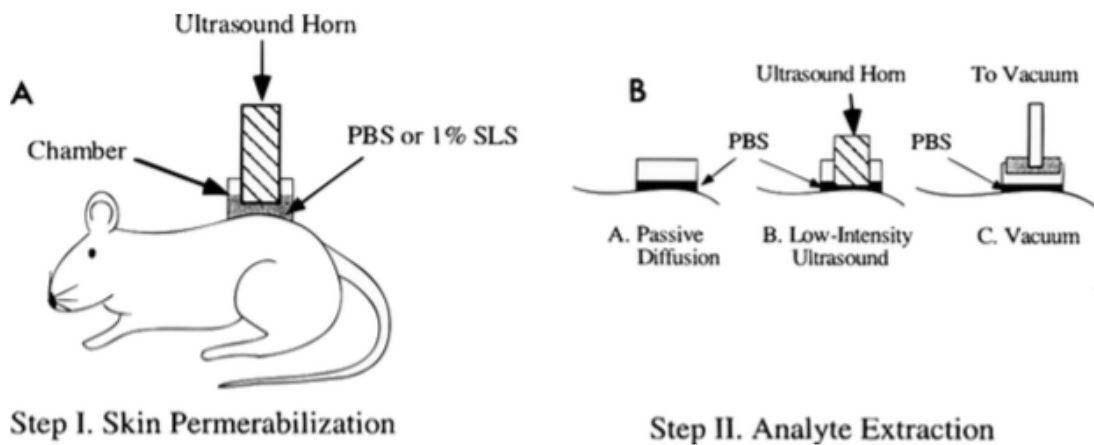


**Figure 6:** A schematic representation of ultrasound application and glucose extraction. (a) shows the application of ultrasound and (b) shows the extraction procedure. Reprinted with permission from Springer.<sup>9</sup>

sonophoresis and has been a primary target of research, especially in the 1990s to early 2000s. While knowledge of sonophoresis has existed since the 1950s, sonophoresis research has been relatively sporadic over the decades.

Sonophoresis is a simple method for delivery and extraction across the SC, but the mode of action is ill-understood despite years of research and modeling. The main theorized mode of action is from cavitation. Cavitation is caused as an ultrasound wave creates a high-density front with a low-density tail through a liquid media. This causes microscopic bubbles to form in the void, which collapse and cause disruption of the SC.<sup>77</sup> Initially, sonophoresis was conducted in the 1-20 MHz range; a frequency that showed an increased transdermal delivery rate of around 100-fold.<sup>78</sup> Further study demonstrated that 1-20 MHz was generally

too fast and that 20-100 kHz yielded a much higher delivery rate.<sup>79</sup> This difference led to the terminologies of High Frequency Sonophoresis (HFS) and Low Frequency Sonophoresis (LSF),<sup>80</sup> the latter of which becoming the predominant form of sonophoresis, encompassing cavitation frequencies of 20-100 kHz.

Sonophoresis is an effective tool for transdermal delivery and has clear clinical applications. HFS has been used to deliver a variety of drugs and chemicals across the skin including hormones, polar and nonpolar organic molecules, and steroids.<sup>78</sup> This permeation of these drugs demonstrates the efficacy of HFS as a tool for increasing SC permeability to a wide range of chemicals in a noninvasive manner. Follow up studies using the same drugs with LSF show increased permeability.<sup>79,81</sup> A more recent review covers the wide range of application for sonophoresis, as well as the frequency and skin model tested.<sup>5</sup>

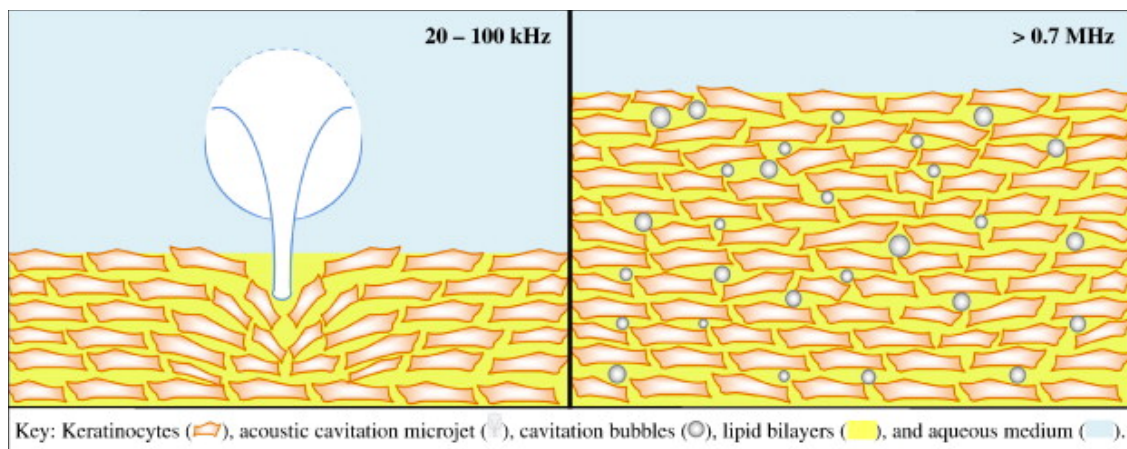


**Figure 7:** (Left) Illustration of cavitation bubble asymmetrically collapsing into the stratum corneum as a microjet under LFS. (Right) Illustration of cavitation bubbles inducing disordering within the stratum corneum under HFS. Reprinted with permission from Elsevier.<sup>5</sup>

Like iontophoresis, sonophoresis has been used to sample ISF contents through a variety of mechanisms. In each literature case, sonophoresis was used to permeate the skin.

This was accomplished by adhering a well to the epidermis, filling the well with a PBS solution, then sonicating the well contents to disrupt the SC; the well contents were then removed and replaced with fresh PBS. The fresh media was then used to either passively

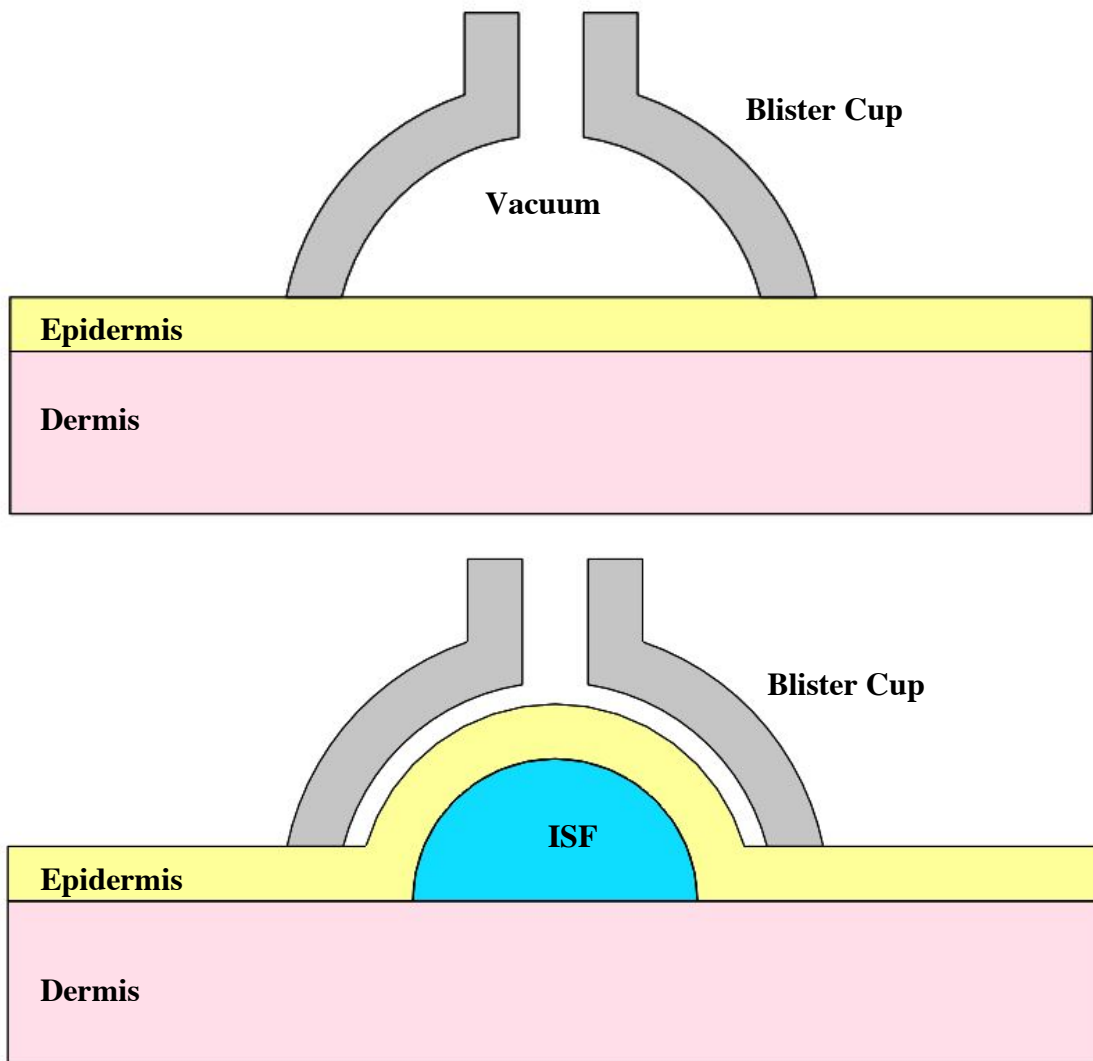


**Figure 8:** Illustration of how the suction blister method delaminates the epidermis from the dermis to create an epidermal blister. Because this method creates a clean boundary between the two layers in which the basal layer is removed from the dermis, it is ideal for ISF analysis as well as skin grafting.

extract ISF through the disturbed SC, using mild ultrasonication to coax ISF from the skin or was placed under vacuum to pull the ISF out manually.<sup>9,81,82</sup> Based on these methods, it was shown that sonophoretic SC disruption increased the permeability by 9-fold under diffusive conditions, 65-fold with mild sonication, and 100-fold with vacuum assistance (based on skin conductance measurements before and after sonication).

The use of a vacuum to extract ISF is one of the most straightforward method of extraction available. Because the subcutaneous interstitial fluid maintains a constant negative pressure, it does not easily seep through the stratum corneum. Vacuum extraction ensures that cells remain held together and that the protective SC maintains contact with the epidermis. The natural negative pressure, however, can be overcome with the external application of an even stronger vacuum.

ISF extraction, through an unexpected side-effect of extended application of a Chinese medicine known as cupping, has been around for at least 3000 years.<sup>83</sup> The original practice of cupping utilizes negative pressure to draw body fluid to the surface of the skin. If too strong of a negative pressure is applied, or if applied for too long, an interstitial fluid blister will form as the epidermis delaminates from the basal layer.<sup>8</sup> While this method is useful for forming skin grafts and making athletes feel more competitive,<sup>84</sup> the suction blister method has been an effective tool for drawing ISF to the surface of the skin for minimally invasive extraction.

Suction blisters have had significant clinical research endeavors pursued since the late 1960s. While primarily researched as a method to generate skin grafts, some studies have been performed to assess the ability of suction blisters to be used for drug metabolism studies. Early studies used drugs such as antibiotics<sup>85-87</sup> to demonstrate the potential utility of blister ISF.

Other studies used drugs that deposit in the epidermis<sup>88</sup> or rapidly distributed nonsteroidal anti-inflammatory drugs.<sup>89,90</sup>

The most notable discoveries from suction blister research, aside from skin grafting, is the advancement of the understanding of various biomarkers within the epidermis. Inflammation around a wound is paramount to healing. Suction blister research has given insight to the effects of anti-psoriatic drug therapy, which can be used to assess immune

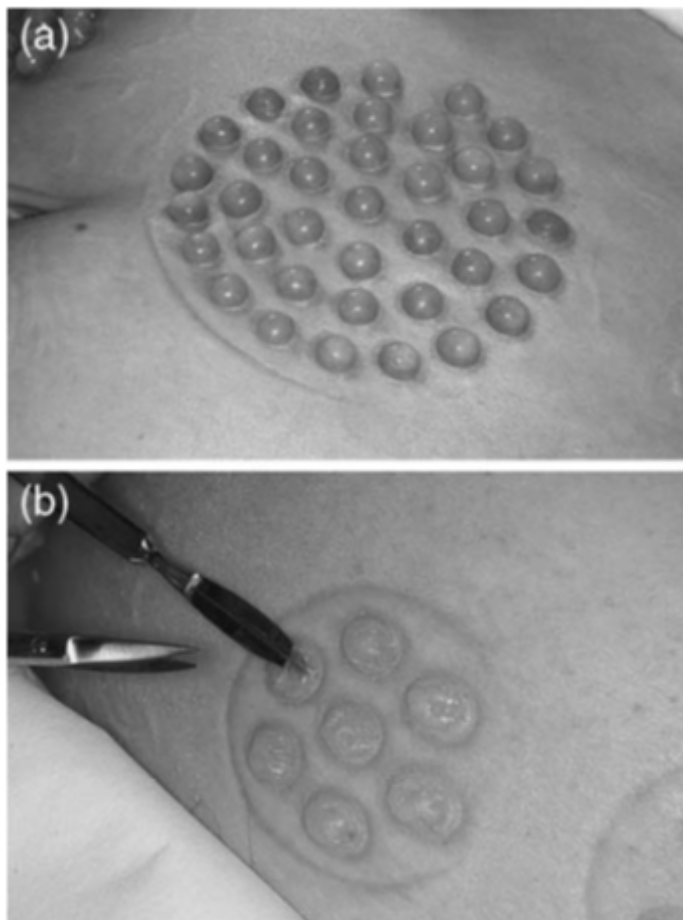


**Figure 9:** (a) Production of suction blisters on lower abdomen with 40 suction blisters measuring 10mm in diameter. (b) Incision of blister. Reprinted with permission from Wiley.<sup>8</sup>

activity,<sup>91</sup> cell regeneration mechanisms,<sup>92</sup> and immune activities.<sup>93,94</sup> While the applicability of the suction blister method may not appeal to many users, the research has demonstrated that suction of ISF to the surface of the skin can be utilized to study key analytes of interest.

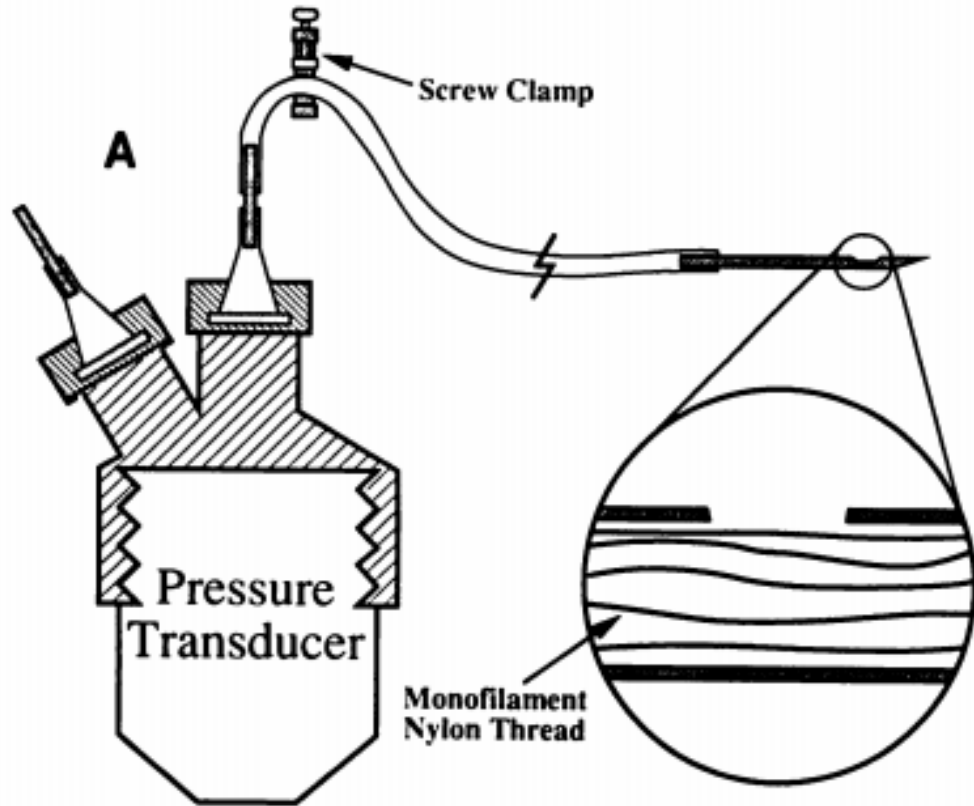


**Figure 10:** The wick-in-needle and pressure transducer setup used for the measurement of interstitial fluid pressure. A 23 gauge needle is built with a 2-3 mm long side hole at 4-5mm from the tip and filled with five nylon sutures. The wick-in-needle is connected via tubing to a needle adapter attached to the dome of the pressure transducer. The screw clamp is used to compress and decompress the tubing in order to test the fluid communication between the transducer and the tumor. Reprinted with permission from the American Association for Cancer

Mechanical and passive pumps (aka wicks) are also possible methods used to access subcutaneous ISF.<sup>95-99</sup> As previously mentioned, transdermal extraction of interstitial fluid requires overcoming a negative pressure. Mechanical pumps are able to overcome a negative

pressure by creating an even stronger negative pressure on the outer surface of the skin. Wicks can overcome slight negative pressures using capillary action.

Wicks utilize capillary action to pull fluid along a route passively and, though demonstrably effective at obtaining interstitial fluid,<sup>97,99</sup> are not suitable for modern medical monitoring, especially outside of a sterile field. Wicks have not been largely used, even in academic settings for two main reasons. First, they require surgical incision and once implanted, result in an open wound with the inability to seal. Second, wicks have been shown to be inaccurate due to nonuniform dilution in the wick.<sup>98,100</sup> The risk to the patient for unreliable monitoring makes wicks more of a crude novelty than a potential component of a medical device.

Pumps, on the other hand, pull fluid using active pressure-modulating machines. Many forms of biomedical pumps currently exist and are commercially available for both fluid absorption and drug delivery.<sup>101,102</sup> Pumps offer an attractive method for ISF extraction, especially with regards to compositional monitoring applications because of their straightforward mode of action and proven efficacy of just that.

There are currently two types of pumps used to monitor ISF contents in the research setting. The first type of pump is called a microdialysis pump and utilizes diffusion across an implanted membrane as a sampling technique. Microdialysis is not a new tool, but has seen several applications in real-time monitoring of select analytes. Because microdialysis operates with a specialized membrane, that membrane can be optimized for selection of specific analytes. Microdialysis has been shown to be useful for analyzing a wide range of compounds over varied durations. Glucose, an ever popular target due to its ease of detection and clinical

impact for diabetics, has been studied continuously for up to three weeks.<sup>103,104</sup> Microdialysis

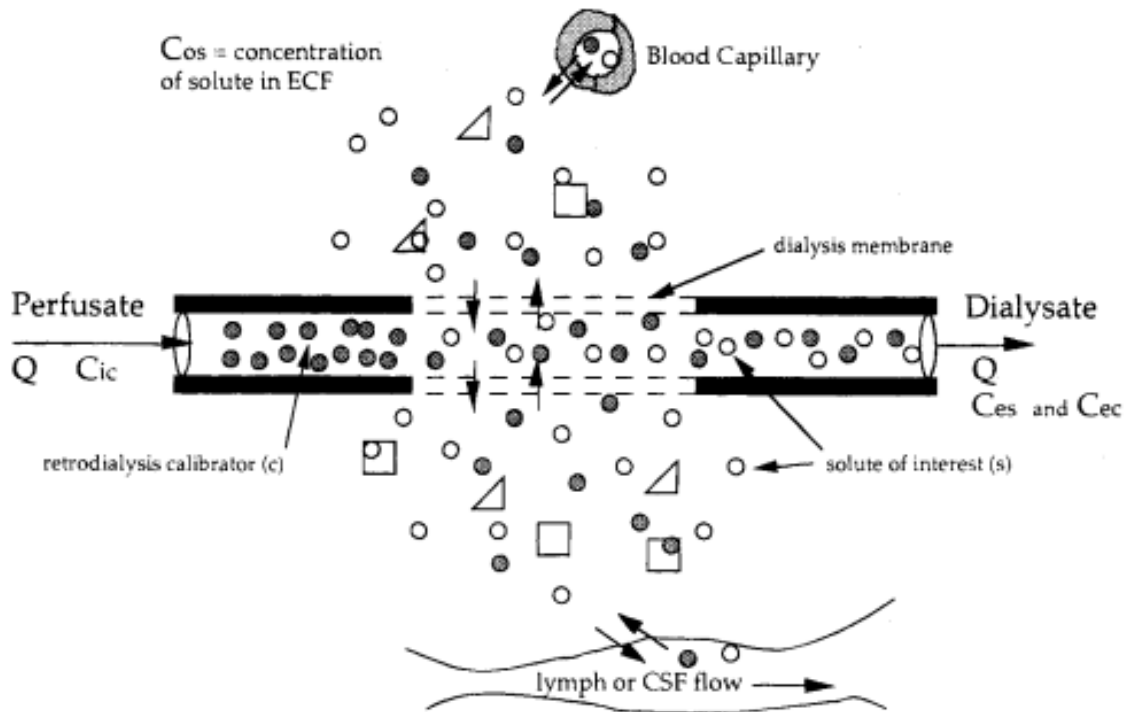


**Figure 11:** Microenvironment within and surrounding the microdialysis probe *in vivo* (not drawn to scale). The solid and dashed line segments schematically represent the nonpermeable probe wall and semipermeable membrane, respectively. Open and closed circles represent the molecules of the solute of interest and a retrodialysis calibrator, respectively. Squares and triangles represent macromolecules which may bind solute and/or calibrator, but which are not recovered by the dialysis process. Arrows indicate direction of mass transport. Reprinted with permission from Springer.<sup>7</sup>

has also been heavily involved with cerebrospinal fluid analysis, targeting amyloid plaque formation as well as other enzymes unique to the environment.<sup>105,106</sup>

The second type of pump is called an open-flow microperfusion pump. Briefly, the pump utilizes convective flow to pull ISF, which freely traverses the implanted probe's porous structure, out of the body in a diluted form. The open nature of the microperfusion pump enables full content analysis of the targeted tissue. Like microdialysis, microperfusion has

been used to study a variety of analytes including glucose, signaling molecules, hormones, and proteins.<sup>107-111</sup> The ability to analyze a wide variety of molecules without biofouling gives microperfusion some perceived advantages over microdialysis, but the dilute nature of the obtained fluid could be a limiting factor of its implementation on the large scale.

Interstitial fluid is a difficult target for continuous analysis for a variety of reasons. Obtaining a pure sample of ISF, free of cells, plasma, or any other contaminate is difficult under any circumstances, never mind for a continuous use application. Fortunately, the past work of countless researchers has provided a solid foundation for continued efforts. While the

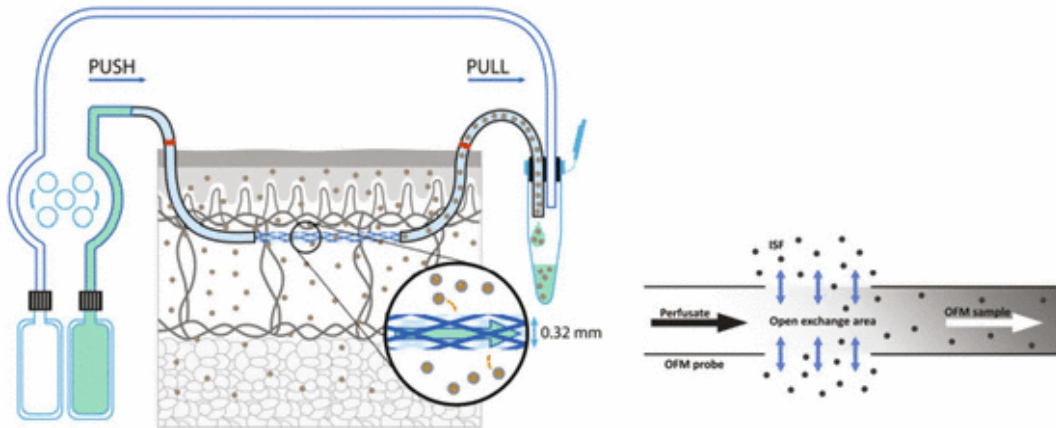


**Figure 12:** Schematic of the open flow microperfusion (OFM) system with a linear membrane-free OFM probe. The inserted OFM probe is connected to a peristaltic pump via push-pull tubing. The OFM pump simultaneously pushes the perfusate into the OFM probe and pulls the OFM sample into and easily exchangable vial. At the exchange area, substances are freely exchanged between the ISF and the perfusate. Image reproduced with permission from SpringerLink.<sup>11</sup>

past work has provided some promising results to build upon, it has also demonstrated some clear obstacles to future investigation of continuous interstitial fluid extraction methods.

One interesting discovery from the use of ISF in metabolic studies is its infrequent correlation with plasma regarding concentrations. While many metabolites and proteins are consistently more concentrated in the plasma, some chemicals pass into the interstitium, leaving high concentrations of the drug in the ISF with little in the blood stream.<sup>88,112</sup> While not an impediment to this project, such abnormalities might confound future applications.

Some of the previous methods of ISF extraction have blatant disadvantages to their implementation. Iontophoresis has demonstrated utility in specific analyte analysis using electrical current to disperse and take-up a wide range of polar and ionic compounds. The technology even had a market presence for a period before the cost of the technology and inaccuracy resulted in its demise.

The use of electricity to move molecules across the stratum corneum requires a continuous direct current. Charging and battery replacement are a major problem associated with patient compliance. While iontophoresis may have its place in a clinical setting, or its place among a specific user group, its reliance on a power source was a hindrance to users while on the market. Furthermore, the only commercially available product, GlucoWatch, was found to cause irritation. This effect is documented and is hypothesized to be due to the effect of ions being forced into proximity to neurons at abnormal concentration,<sup>35</sup> making iontophoresis unsuitable for long-term continuous use.

Of the methods of ISF sampling listed, sonophoresis is the least practical. Although it has been shown to be effective at distorting the SC in such a way as to allow trans-membrane movement, it requires a complicated setup with fluid wells adhered to the body and an external sonic generator. In addition, it has been shown that sonophoresis is not as effective as other

methods for extraction of interstitial fluid and is best suited for use in addition to other methods, such as iontophoresis or pump assisted extraction.

External suction methods like the suction blister method mechanical pumping have provided a great wealth of knowledge regarding ISF extraction. The suction blister method, although not visually appealing, has provided the best representation of ISF composition with minimally invasive extraction techniques. While the suction blister method is effective at extraction of interstitial fluid, its use is not practical for continuous analysis due to the inability to form a continuous blister. To create a continuous flow of interstitial fluid for analysis, an external pump must be implemented.

The external pumps reviewed here do not represent the full extent of the applicability of ISF pumps, but do demonstrate a few methods for ISF extraction. It is important to note that these pumps all function as implantable devices, and are therefore relatively invasive. As implanted devices, they are subject to biofouling and put the user at risk for infection at the implant site.

While the listed extraction devices are effective for obtaining ISF through arguably non-invasive methods, they do not function well for continuous at-home use, which is a major industrial target for health monitoring systems. New research however has the potential to advance this effort by combining some of the attributes of these methods in the use of microneedle based pumps.<sup>113</sup>

## **Microneedles**

Blood sampling is a painful process requiring needle sticks, which puncture the protective stratum corneum. Nociceptors, located just below the epidermis, cause pain signals to transfer to the brain upon puncturing of the skin.<sup>114</sup> The brain, in response to the nociceptor signals, triggers an immune response. This cause and effect flow is not only physically painful and ill-received by the patient, breaching the stratum corneum puts patients at risk for infection.<sup>115-117</sup> Immunocompromised populations, including children, the elderly, those taking immune suppressing drugs, or those suffering from immune disorders are at elevated risks for infection and are the populations most commonly getting blood sampled or getting injection-based therapy. Microneedles have potential applications in pain-free ISF extraction and could potentially be used for continuous monitoring of ISF analytes.

Microneedles are devices with a wide variety of applications with an equally wide variety of qualifications for what defines a microneedle. For this work, a microneedle will be qualified as a needle-like structure with an overall length of less than 1mm. Aside from size, microneedles can come in a variety of shapes, thicknesses, etc. and have a variety of functions. Although microneedles were originally used as tools for micromanipulation, their uses have recently become of interest to the pharmaceutical and medical device industry.

The structure of the epidermis is the basis for the applicability of microneedles, especially regarding pain and patient compliance. Because the pain receptors, primarily A $\delta$  nociceptors, reside below the epidermis, microneedles are not able to induce a pain response. This has made microneedle-based devices a modern target for drug delivery and health monitoring applications.

The ability to access the interstitium without causing pain and/or inflammation for an extended duration has been the target of transdermal drug delivery systems for years, but has yet to be achieved on the industrial scale. Efforts towards making microneedles a viable device for interstitial fluid extraction, like previous attempts, have begun to rise from attempts at using microneedles for drug delivery.

## **HISTORY**

Microneedles have been an area of study for a significant part of the past century, starting with single glass needle fabrication in 1952 using hydrofluoric acid.<sup>118</sup> Although microneedles were an area of focused research, they did not gain much biological significance until the late 1960s, when microneedles found use in insect studies.<sup>119</sup> Still, these devices did not receive much attention from the biomedical community until the turn of the century, when their potential in drug delivery applications became an intense area of focus.<sup>120-123</sup>

Shortly after the turn of the century, microneedle structures and materials began to evolve. The fragile glass and silicone needles gave way to metal needles,<sup>124</sup> solid needles were given hollow channels as a way to pump fluid across the SC instead of passively diffusing across a punctured SC,<sup>124-126</sup> porous needles were investigated as potential delivery devices,<sup>127</sup> and investigations into the efficacy of microneedles as transdermal delivery devices validated the devices as potentially relevant research targets.<sup>128,129</sup> Since the early 2000s there has been a surge in research efforts aimed at creating cheap and effective drug delivery vehicles. The increased activity has yielded vast amounts of data on microneedle design, materials, drug delivery, and more.

Early microneedles were initially formed from pulled glass for microscale manipulations. The pulling process is still used, but is very time intensive for little output and has limited applicability in a wearable device. To create biologically purposed microneedles, polymeric microneedle arrays were developed as delivery vehicles.

M. Prausnitz is given credit for developing the first microneedle array for drug delivery in 1998.<sup>121</sup> The early push for microneedle development stemmed from the need to create transdermal delivery methods that circumvented the natural impermeability of the stratum corneum. The initial significance of the early designs revolved around the puncturing of the stratum corneum to increase permeability of topical creams.<sup>61,121,126</sup>

Simple puncturing of the stratum corneum was accomplished through relatively straight forward methods. Solid and hollow microneedles made of glass and metal were the initial materials of interest<sup>124,130</sup> as they are both strong materials that can easily pierce the skin. Glass however has been a concern as broken needles left in the skin could lead to infection, encapsulation, and other health concerns.

Silicon microneedles, fabricated with photolithography and ion etching<sup>124,131</sup> are incredibly sharp and have proven effective at piercing the skin, but are very expensive to manufacture.<sup>132,133</sup> While these needles definitely have a wide variety of uses, they would not be the desired material for a disposable and continuous monitoring device. To create such devices, materials and manufacturing costs must be minimal. Fortunately, synthesis of polymeric microneedles can address the problem of expense.

As research endeavors progressed, microneedles became a target all-in-one delivery concept, which led to a variety of designs. Since the realization of microneedle devices as

medical devices, research efforts have produced a wide variety of needle shapes and sizes from a wide variety of dissimilar materials, each tailored to specific applications.

### **Microneedle Design**

As in many aspects of the natural world, structure, form, and function all work together in tandem. Microneedle function is the primary determinant of structure and form. As mentioned before, microneedles gained initial interest as a device for piercing the stratum corneum to leave holes and increase drug permeation. Solid silicon<sup>134,135</sup> and steel<sup>128,136,137</sup> microneedles can be reused and are effective at pore formation in the SC to improve transdermal drug delivery. Now, these devices have market value as “derma-rollers,” used for improving skin clarity, though clinical application shows little efficacy.<sup>138</sup> Solid coated silicon and steel microneedles have also been used to deliver molecules across the SC instead of being used solely to perforate the barrier layer.<sup>121,139</sup> These materials, as well as polymeric microneedles, have also been fabricated into hollow-bore<sup>125,140</sup> and out-of-plane-bored needles.<sup>131</sup> Hollow microneedles enable fluid exchange, an important feature for sustained delivery or extraction of fluid across the stratum corneum. The continuous research into microneedle design has led to the development of five main classes of microneedles in relation to their modes of action: solid microneedle “poke and patch,” “coat and poke,” dissolving, hollow-bore, and hydrogel.<sup>12</sup> These designs will be evaluated briefly for pros and cons of the

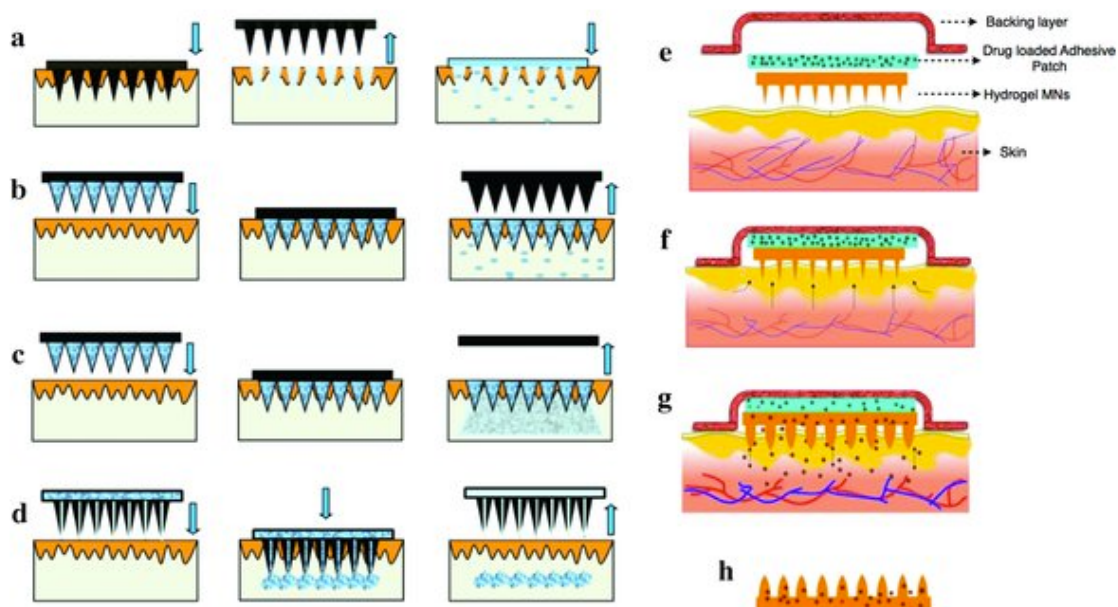


**Figure 13:** Schematic representation of methods of MN application to the skin to achieve enhanced transdermal drug delivery. a–d) Traditional methods of MN-mediated drug delivery across skin. (a) uses solid MN that are applied and removed to create transient micropores, followed by application of a traditional transdermal patch. (b) uses solid MN coated with drug for instant delivery. MN are removed after coating material dissolves. (c) uses soluble polymeric/carbohydrate MN containing drug that dissolve in skin interstitial fluid over time, thereby delivering the drug. (d) uses hollow MN for delivery of fluids containing drug. e–h) Our novel hydrogel-forming polymeric MN for controlled transdermal drug delivery. (e) shows an exploded view of our novel integrated hydrogel MN patch, which consists of a backing layer, a drug-loaded adhesive patch and a solid crosslinked hydrogel MN array. (f) shows application of the integrated hydrogel MN patch to the skin surface. This is followed by diffusion of water into the crosslinked integrated MN patch. (g) shows diffusion of water, which causes controlled swelling of the MN arrays, forming an in situ hydrogel conduit. This further results in liberation and diffusion of drug molecules from the adhesive patch through the hydrogel MN into the skin. (h) shows that the hydrogel MN arrays remain intact, even after removal from the skin, thereby leaving no polymeric material in the skin following drug delivery. Figure reprinted with permission from John Wiley & Sons<sup>12</sup>

general designs and materials used, but **Figure 13** offers a schematic for each respective mode of action.

Solid MNs are the foundation of microneedle research. They are abundantly researched and have a wide variety of applications. Currently, stainless steel is one of the primary materials used for microneedle manufacturing, owing to its medical history as a biocompatible metal.<sup>141</sup> Stainless steel is an easy and durable material to machine into microneedles using AutoCAD software and laser etching techniques,<sup>142</sup> which has made it a feasible material for industrial use. Currently, several companies sell what is known as a Dermaroller®, a barrel coated with microneedles used for various applications. Dermarollers® have been used cosmetically<sup>134,138,143-146</sup> as a means to increase topical delivery of therapeutics via pore formation, or on their own to promote growth factor development and promote collagen formation.

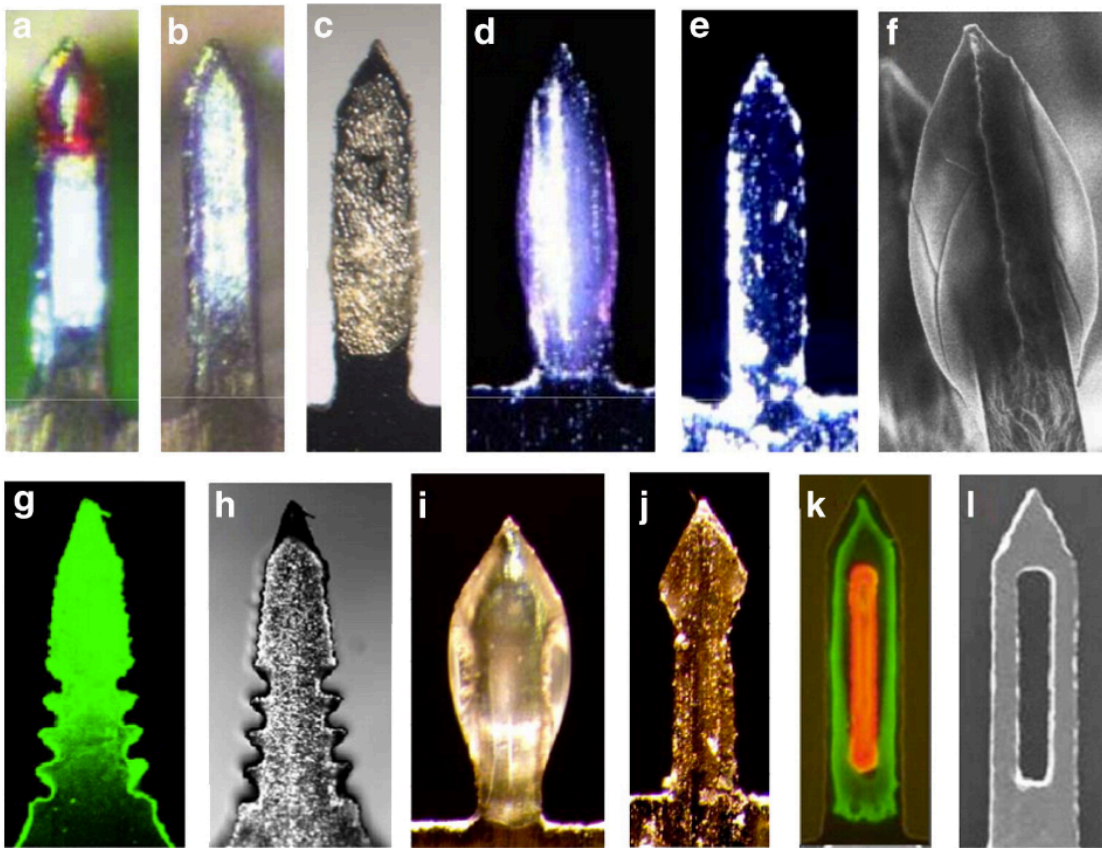


**Figure 14:** Varieties of microneedles before coating (b, d, f, h, j, & l) and after coating (a, c, e, g, i, & k). Reprinted with permission from Elsevier.<sup>4</sup>

A study by Donnelly et al. demonstrates that micro perforation of the skin can be used to deliver more effective photodynamic therapy. Briefly, excised skin was perforated using solid silicon microneedles. Perforated and non-perforated skins were compared in a Franz cell as patches of 5-aminolevulinic acid was administered as a transdermal film. The study shows that perforation is an effective way to increase drug permeation.<sup>134</sup>

Coating solid microneedles also has several therapeutic applications for drug delivery. These microneedles have demonstrated viability for delivering potent peptide drugs, which are often administered as an injectable, orally, or transmucosally. While injection is the preferred method of administration over oral and transmucosal routes, which severely hinder bioavailability,<sup>147</sup> it is a painful and unsuitable vector in children. **Figure 14** shows the optical differences in uncoated and coated microneedles. One study utilized desmopressin as a model coating drug and identified a consistent delivery of 10%.<sup>148</sup> While not very useful in terms of delivery efficiency, the delivery was demonstrated to be tunable and repeatable for physiological relevance ( $\sim 20\mu\text{g}$ ).

Prausnitz et al. have also conducted a very thorough investigation of various target molecules for TDD using solid MNs as well as a variety of shaped needles. His group demonstrated the utility of laser-cut stainless steel microneedles with pockets that could deliver a wide range of compounds: sulforhodamine and calcein (large lipophobic dyes), Texas Red tagged BSA (protein), tagged plasmid DNA, vaccinia virus, and nanoparticles up to  $20\mu\text{m}$  in

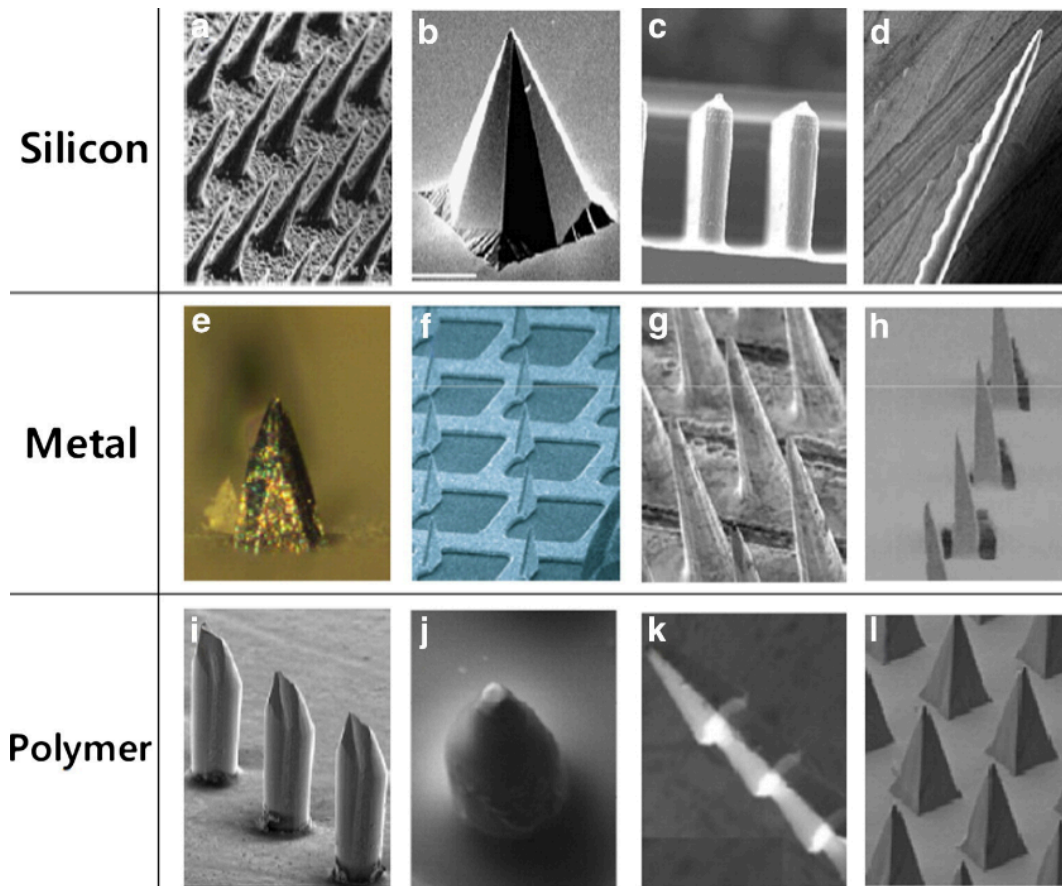


**Figure 15:** Examples of solid microneedle designs based on materials. Reprinted with permission from Elsevier.<sup>4</sup>

diameter.<sup>142</sup> The delivery of DNA, vaccinia virus, and nanoparticles to a targeted area without hypodermic needles represents a huge potential of applications for solid coated microneedles.

While solid microneedles can be easily fabricated into a wide range of shapes and used to deliver a plethora of therapeutics, they do suffer from some drawbacks that make them unsuitable for certain applications, such as applications in which outward flow is desired.

Fabrication of hollow bore microneedles were designed to act as channels through the stratum corneum. Hollow-bore microneedles are often utilized in tandem with pumps and reservoirs for introduction of fluids across the SC,<sup>149-153</sup> but they have also been attached to pumps that withdraw ISF.<sup>4</sup> Since hollow-bore microneedles are the simplest method to deliver a continuous flow across the stratum corneum, it is not surprising that a plethora of hollow-bore needle designs have been developed; **Figure 16** provides some examples of recent designs. While hollow-bore microneedle applications with external pumps is relatively straightforward, one of the major pushes for future microneedle devices is self-containment to improve patient compliance.

As described above, solid microneedles have been shown to effectively deliver a wide range of compounds across the SC. While effective, these designs are limited by surface area

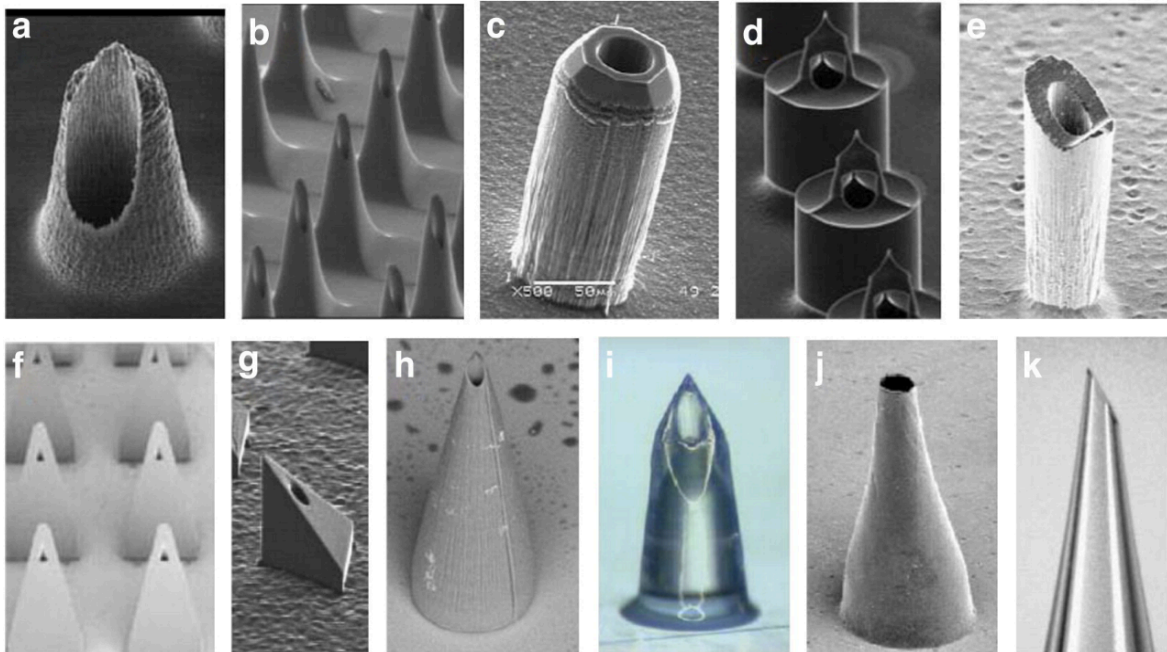


**Figure 16:** Examples of hollow-bore microneedles. Reprinted with permission from Elsevier.<sup>4</sup>

in terms of delivery volume. Hydrogel and dissolving microneedles have been developed and evaluated as potential devices that could deliver larger doses and, in the case of hydrogels, be used similarly to hollow-bored microneedles for continuous delivery.

Dissolving microneedles are conveniently designed needles that could enable delivery of large doses across the stratum corneum. When compared to solid needles, dissolving microneedles have the full volume of the needle available to deliver the payload, as opposed to just the surface area. Dissolving microneedles have been fabricated from albumen, chondroitin sulfate, dextran and have been effective at delivering erythropoietin, a signaling protein as well as several other compounds.<sup>154</sup> **Figure 17** displays a few of the developed microneedles designed to dissolve to release therapeutics.

These types of needles have also been fabricated from other biopolymers. In 2008, Prausnitz et al. developed microneedles from carboxymethylcellulose and amylopectin for the storage and delivery of sulforhodamine B, BSA, and lysozyme. The lysozyme was demonstrated to be shelf stable for 2 months at room temperature once encapsulated within the microneedles.<sup>155</sup>

Continued experimentation resulted in further evidence that biomaterials, including sugars, polysaccharides, and proteins were all effective at delivering a wide range of molecules ranging from vaccines to proteins, to drugs and other small molecules.<sup>156-159</sup> While these

advances are important, the dissolution of microneedles in order to deliver a larger payload is not always necessary.

Hydrogel-based microneedles are cast from a solution, much like soluble microneedles, but are crosslinked such that the needles, once inserted, swell with interstitial fluid and enable flux through the main body of the needle. This type of device creates what Donnelly describes as “continuous, unblockable hydrogel conduits...to the dermal microcirculation.”<sup>12</sup>

Hydrogel microneedles, unlike hollow-bore needles, cannot be blocked as they puncture skin because they do not have intrinsic holes in which to block flow. Instead, they enter as a solid microneedle then swell to create a channel, thereby enabling continuous

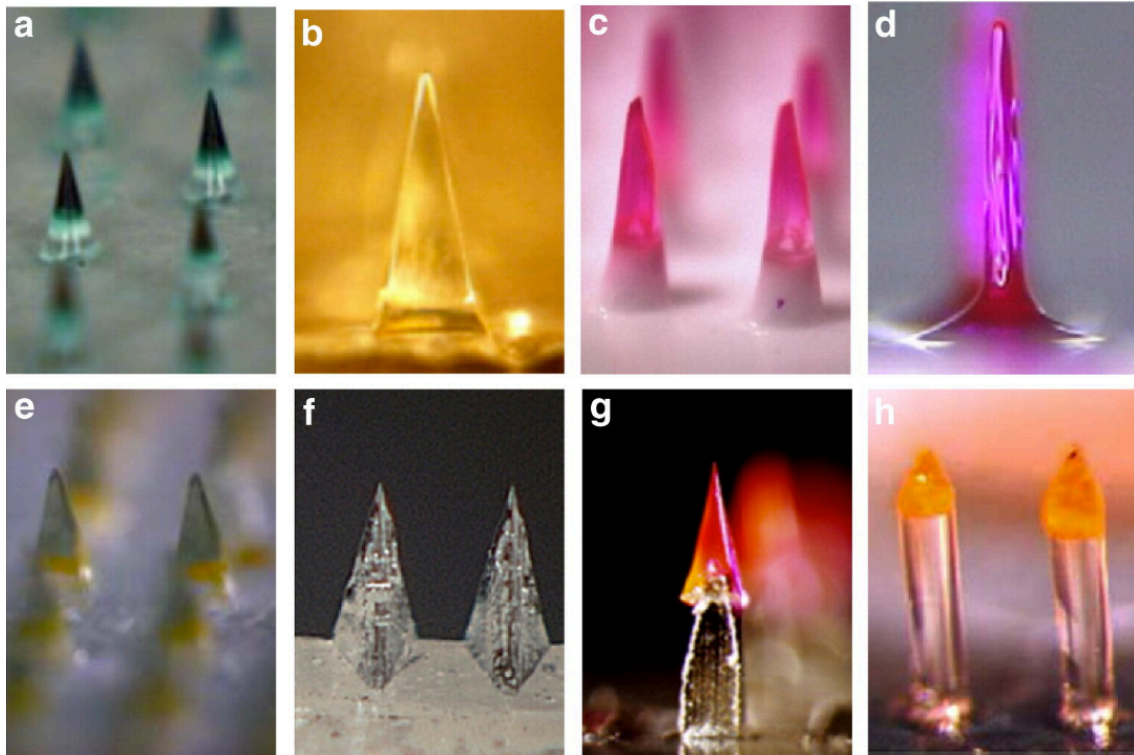


**Figure 17:** Examples of dissolving microneedle delivery systems. Reproduced with permission from Elsevier

transport across the SC. The unique properties of hydrogel microneedles could open an even broader range of applications for microneedles in clinical, OTC, or patient monitoring applications.

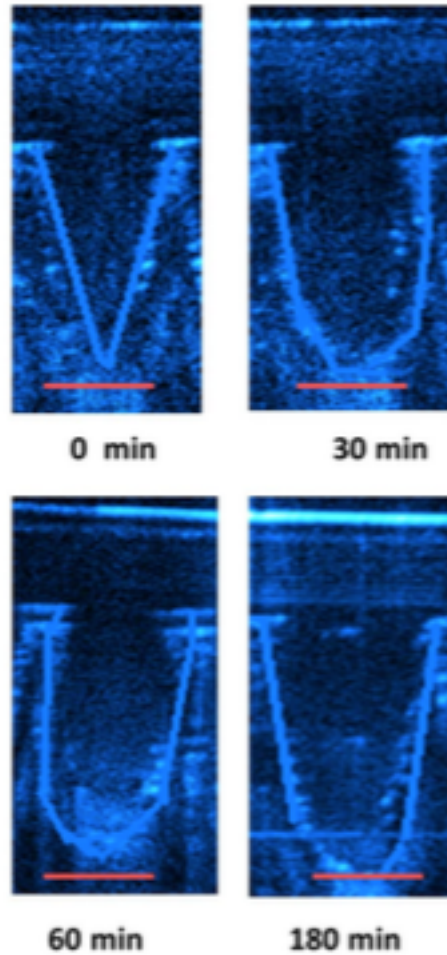


**Figure 18:** Gantrez-AN-139/PEG hydrogel microneedles inserted into neonatal porcine skin and imaged with OCT immediately following insertion. Scale bar represents 300 $\mu$ m in each image. Reprinted with permission from PloSOne.<sup>10</sup>

Many research efforts in hydrogel-based microneedle development rely on synthetic polymers, such as polyacrylates, polyacrylamides, methyl vinyl ethers, and PEGs.<sup>10,160,161</sup> These materials are all highly hydrophilic and swell greatly. Furthermore, they have been used for the delivery of a litany of drugs including donepezil (Alzheimer's disease),<sup>162</sup> insulin,<sup>160</sup> and ibuprofen.<sup>10</sup> While dose volume is still a limiting problem in microneedle applications, the open structure of hydrogel microneedles has the potential to address the issue. Because the microneedle acts as an open channel for passive diffusion, it has been proposed that a passive well could be advantageous for the delivery of higher doses over a longer period.<sup>151</sup>

Conveniently, as seen repeatedly with other delivery methods, these hydrogel-based microneedles also act as a channel to extract interstitial fluid for analysis. The use of microneedles in this way is exceptionally new, with the first publication being less than two years old.<sup>76</sup> This paper demonstrates the ability of poly(methyl-vinylether)/PEG composite microneedles to absorb theophylline, caffeine, and glucose both *in vitro* and *in vivo* using mouse and human models. These microneedles, along with other attempts,<sup>113,163</sup> have shown microneedle use in absorbing analytes from ISF or ISF-like solutions. These studies, however, do require the microneedle array to be analyzed by extracting the analytes back from the needle and do not demonstrate real-time utility of the devices for compositional analysis.

## **Conclusion**

A large majority of microneedle research has been geared towards development of solid metal and silicon microneedles. These materials can be manufactured in a variety of shapes and dimensions to achieve certain goals. While these materials are incredibly strong and can

easily puncture the skin, they are predominantly solid. Solid microneedles are suitable for drug delivery and perforation of the stratum corneum, but their capabilities of drug delivery are limited by to the surface area of the microneedle.

These needle materials can be designed in ways that increase their surface area through pitting or putting holes in the needles as pockets, but the major drawback of using metal and silicon is the cost of manufacturing. Ion etching and high precision laser use is very expensive but is the primary methods used to form these types of microneedles. Intricate designs, such as hollow-bore needles or out-of-plane hollow needles dramatically increase the difficulty of production.

Hollow-bore microneedles are very effective at creating channels across the SC and have demonstrated their use in both delivery and extraction across the barrier. These designs can be manufactured from both inorganics, like metal and silicon, and organic polymers, like PVA or PMMA. The ability to create these needles from a variety of materials gives rise to application variety. At home use with disposable polymeric microneedles could provide a cheap pain free alternative for delivery or testing, while inorganic microneedles could be sterilized in a clinical setting for repeated use, thereby justifying their higher cost.

The main drawbacks with regards to hollow-bore microneedles come from their potential for obstruction and their need for external pumps. As mentioned earlier, out-of-plane bores have the potential to compensate for obstruction during insertion but is only possible through complex design and fabrication techniques. Obstruction could lead to poor function of the microneedle device and could negate the main purpose.

Hydrogel microneedles, although still new materials for research, seem to combine the attributes of both solid and hollow microneedles while minimizing their problems. Production of hydrogel microneedles is simple, only requiring a mold. The needles can be fabricated from a wide variety of polymers, can be used to encapsulate a list of compounds ranging from small molecules to nanoparticles for delivery upon insertion, and can be used in similar fashion to hollow-bore microneedles for delivery.

### **Significance of Project**

Microneedles have been a serious focus for research endeavors ever since their fabrication was made possible in the 1990s. Due to the great demand for pain-free delivery methods to increase patient compliance, microneedle research has been geared towards drug delivery applications. The ability to deliver vaccines, proteins, and regulating molecules to patients without puncturing their skin could not only improve patient compliance, but also limit the volume of patients who acquire infections through needle sticks.

Historical observation has demonstrated repeatedly that many transdermal drug delivery methods can be engineered to work in reverse to extract interstitial fluid. Interstitial fluid closely resembles blood plasma and has been a target for body composition research for decades. Despite a large scientific push to develop methods for extracting ISF, it remains a difficult target.

Not coincidentally, the two research fronts have begun to overlap in the past decade. The desire to create open pores across the stratum corneum for continuous delivery of therapeutic molecules attracted attention from engineers seeking to extract ISF. Initial works

made use of the inorganic hollow-bore microneedles to pump ISF out of the body for analysis. This method is clearly inconvenient, requiring external pumps, collection vessels, external analysis, and more.

Development of hydrogel-based microneedles for delivery of larger volumes of drug enabled further exploration of microneedle material options. While these designs have been moderately investigated for their delivery potentials, field leaders Prausnitz and Donnelly have pushed the limits for the devices and have demonstrated their ability to absorb ISF. Their work shows that hydrogel microneedles can be used to painlessly extract ISF without the use of external devices.<sup>10,113,163</sup>

Despite this breakthrough, there are still advances to be made for this class of microneedle. The current state-of-the-art shows little functional independence of the devices, requiring absorption analytes to be analyzed on external HPLC with technical precision by trained scientists. While this may be feasible in a clinical setting, its use in the field would be restricted and would not provide the continuous monitoring device necessary in the age of the quantified self.

To create a technology that can add substantial benefit to man in the form of continuous quantification, it is proposed that similar hydrogel microneedles can be utilized with a passive pump to continuously extract interstitial fluid. To further the advancement of the technology for real-world application, it is conceived that such a device could function in conjunction with an optical sensor to provide a wearable, continuous, real-time monitoring device for specific quantification of target analytes.

This work focuses on the development of a continuous ISF extraction device with continuous sensing in mind. To achieve such goals, emphasis is placed on the development of hydrogel microneedles with wicking properties. This work utilized a unique biopolymer called hyaluronic acid as the basis for microneedle fabrication. Hyaluronic acid is the highly abundant and hydroscopic polymer found in the extracellular matrix. Its semblance to the ECM and natural presence therein make it a highly biocompatible material for extended use applications.

Due to the negative pressure associated with subcutaneous ISF, addition of cellulose to the hyaluronic acid microneedles is proposed as a method to wick ISF from beneath the stratum corneum. Integration of cellulose with the needle array and adherence of the array to a cellulose-based paper pump is hypothesized to be an effective method to produce a prototype device as described above.

Fabrication of an all-in-one sensory device with optical sensors could provide physicians, patients, and hobbyists the means necessary to quantify body composition of a periodic scale, more frequently, without the pain associated with needles and without the need for blood work. Furthermore, development of this technology will reduce the risk of infections from frequent needle sticks, which will reduce the accidental needles stick rate in hospital staff and home-users. The combination of which could save the medical industry billions of dollars and the innumerable man hours spend dealing with infections and accidental exposures.

## **Detailed Synopsis**

### *Microneedle Materials:*

The proposed device will be intended to operate as a continuous monitoring device over the course of a day before disposal. As such, it is important that the use of the device minimizes potential for immune response, especially after repeated exposures. To prevent negative consequence of continuously using microneedles, hyaluronic acid was used as a foundation material.

Hyaluronic acid is a disaccharide-based polymer consisting of D-glucuronic acid and N-acetyl-D-glucosamine linked with alternating  $\beta$ -(1  $\rightarrow$  4) and  $\beta$ -(1  $\rightarrow$  3) glycosidic bonds.

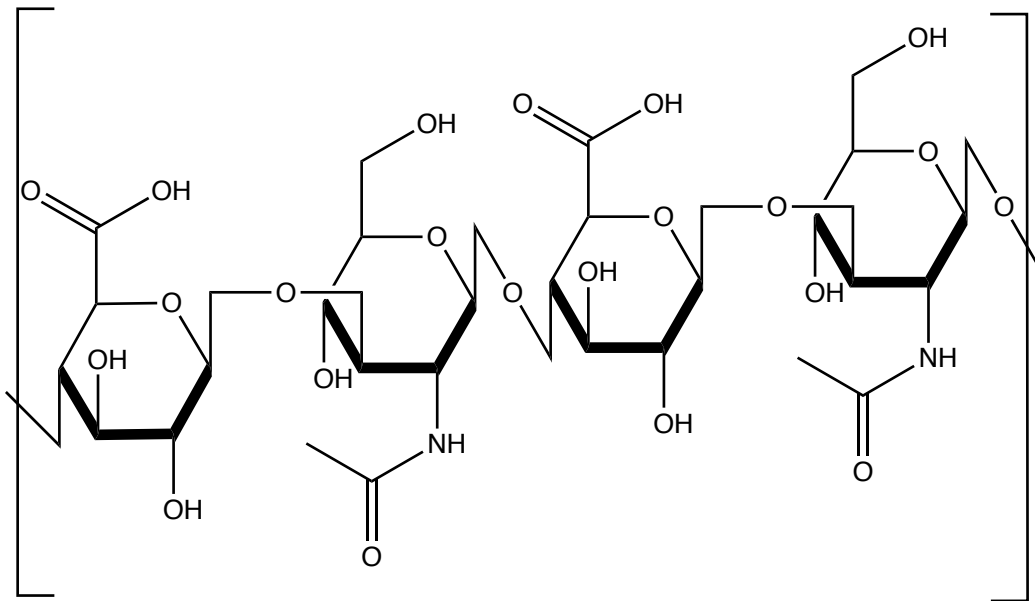


**Figure 19:** Hayworth projection of hyaluronic acid.

HA is a natural component of the extracellular matrix and is important in maintaining many aspects of cellular function, one of which being wound maintenance.

Hyaluronic acid, being a biologically produced polymer, can be broken down by the hyaluronidase class of enzymes. These enzymes cleave the N-acetyl-glucosamine / glucuronate bonds into subunits, which trigger angiogenesis.<sup>164</sup> By using a material that is

biologically inert at high weight and beneficial when degraded, it is assumed that immunogenic reactions will be minimized, even after extended use.

Hyaluronic acid is a water-soluble biopolymer with a variety of reactive groups, including amines, hydroxyls, and carboxylates. The variety of functional groups enable HA to be crosslinked in a variety of ways including amide formation and ester formation. These functional groups make it possible to do more complex reactions to attach a wide range of functional handles for an endless list of crosslinking.<sup>165</sup>

One popular method used for forming esters and amides is through carbodiimide initiators. Carbodiimides crosslink carboxyl groups to alcohols and amines through isourea intermediates under mild conditions with often soluble urea byproducts. In biomedical

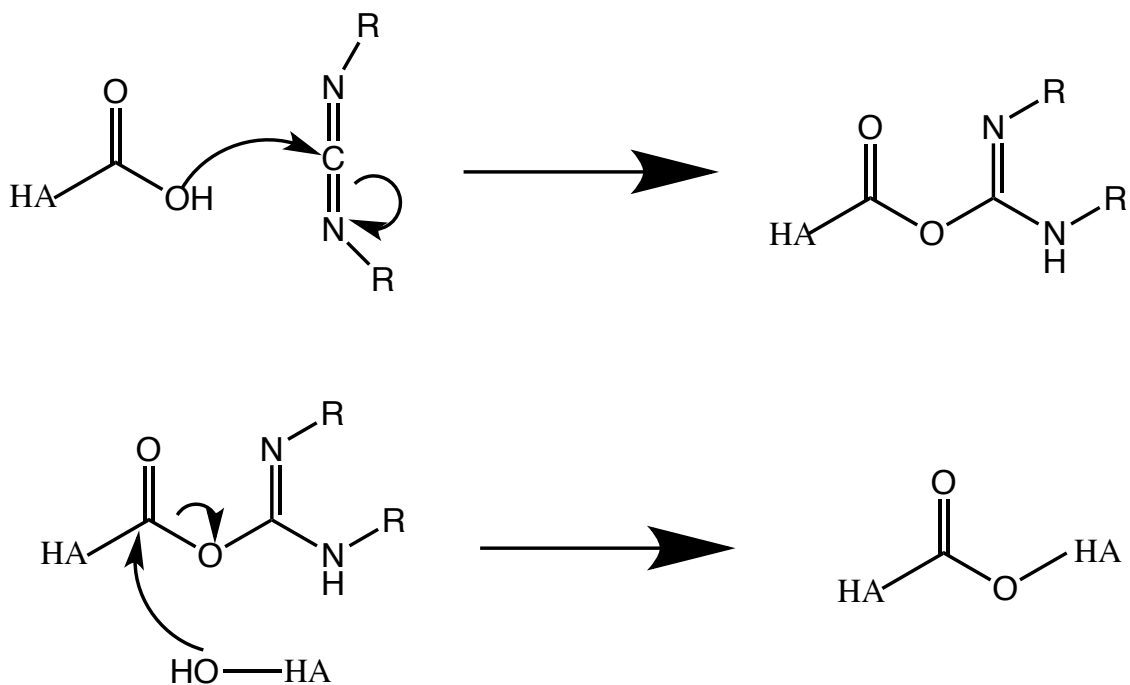


**Figure 20:** Informal mechanism describing the carbodiimide crosslinking reaction of HA

applications, it is paramount that residual byproducts do not harm the patient or user, so this property makes it an ideal crosslinking agent for internal applications.

The goal of this project is to form a microneedle array, traversing the stratum corneum, for extended use. To accomplish this, it is hypothesized that crosslinking hyaluronic acid to itself, using a crosslinking agent that forms few byproducts with minimal risk of immunogenic response. This work relies on the use of EDC (1-ethyl-3-(3-dimethylaminopropyl)carbodiimide hydrochloride as a crosslinker because it is water soluble and has been proven to work in dilute aqueous solutions, which is key to crosslinking dried, water soluble polymers.<sup>166</sup>

#### *Absorbance:*

Because hydrogels contract as they dry, it is important that the dry crosslinked needles absorb fluid and expand into a wide network capable of taking on several times their initial volume in water. By absorbing and swelling, hydrogel microneedles effectively disappear into the ISF while creating an open channel across the stratum corneum. Given an external force, the hydrogel becomes a conduit through which ISF can be extracted.

To assess the abilities of the HA-based hydrogels to act as such a conduit, cast films of the hydrogel can be used to assess the overall amount of fluid the gels can absorb. High water absorbance would indicate the hydrogel has potential to act a channel with minimal obstruction and that the network does indeed expand to accommodate the influx of water.

Microneedles can also be evaluated for their ability to swell using a variety of methods. Swelling in three dimensions is necessary to minimize obstruction of flow across the stratum

corneum. As a network expands in volume, the polymer chains spread apart until an equilibrium is obtained. Comparing the 2D vs 3D swelling between HA and HA-cellulose composites could provide insight as to whether addition of cellulose increases the ability of the microneedles to absorb water (e.g. higher 2D water absorbance with similar 3D expansion would indicate higher water affinity).

*Mechanical Testing:*

Mechanical testing of developed microneedles offer insight to their structure, but ultimately determine if they are suitable for the intended purpose. The purpose for most microneedles is to puncture the stratum corneum without causing pain. While the geometry of

**Table 1:** Foundational equations for consideration when designing microneedles.

Equation Number	Formula	Description
(1)	$F_{MC} = \sigma_y A$	Max Compressive Force: $\sigma_y$ is the material fracture strength and A is the cross-sectional area
(2)	$F_{MB} = \frac{C\pi^2 EI}{L^2}$	Max Buckling Force: C is a condition constant equal to 0.25, E is the Young's modulus of the material, I is the moment of inertia related to the microneedle geometry, and L is the length of the microneedle
<u>Microneedle Geometry</u>		<u>Moment of Inertia</u>
	Circular*	$I = \frac{1}{64}\pi D^4 - \pi d^4$
	Rectangular*	$I = \frac{1}{12}BD^4 - bd^4$
	Square*	$I = \frac{1}{12}HD^4 - h^4$
(3)	$F_{MFB} = \frac{\sigma_y I}{cL}$	Free Bending Force: c represents the distance from the neutral axis to the outer edge of the microneedle
(4)	$F_{MCB} = \frac{2\sigma_y I}{cL}$	Constrained Bending Force: Bending force once the microneedle has punctured the skin.
(5)	$F_{MS} = \frac{\sigma_y A}{2}$	Shear Force: The perpendicular force experienced at the base of the microneedle once inserted into the skin
(6)	$F_{SP} = P_{Pierce} A$	Skin Resistance: The resistive force of the skin. A is the cross sectional area of the skin

\* Capitalized variables are the outer diameters of the microneedle while lower cased letters represent the diameter of internal microchannel of the microneedle

the needles may be easy to manipulate, if the materials do not have the required strength to pierce the SC, the needles have no practical utility.

Needle shape, size, and spacing were all taken into account due to their effect on mechanical strength.<sup>167</sup> Six factors must be accounted for: compressive force, buckling force, free bending force, constrained bending force, shear force, and the resistance of skin to puncture. These can be calculated from the equations 1-6, respectively.

These simple equations can be expanded into complex mathematical examinations of the microneedle-skin deformation, but such examination is outside the scope of this project. Using piezoelectric sensing, it has been determined that puncturing of the stratum corneum with microneedles is sufficient using 0.1-3N of force.<sup>140</sup> Therefore, it is an important goal that the developed HA microneedles have a max compressive force and max buckling force greater than 3N and, ideally, greater than 6N.

## **Materials & Methods:**

### **Materials:**

Hyaluronic Acid sodium salt from *Streptococcus equi* (Sigma-Aldrich, product#: 53747), N-(3-Dimethylaminopropyl)-N'-ethylcarbodiimide hydrochloride (Sigma-Aldrich, product#: E7750), Sodium Azide (Sigma-Aldrich, product#: S2002), N-Hydroxysuccinimide (Sigma-Aldrich, product#: 130672), Sodium Phosphate Dibasic (Sigma-Aldrich, product#: S3264), Bacto-Peptone (BD, product#: 211677), Citric Acid Monohydrate (VWR, product#: 0908), Yeast Extract (Alfa Aesar, product#: J60287), Dextrose Anhydrous (BDH, product#:

BDH9230), Cellulose Nanofibrils – TEMPO (The University of Maine Process Development Center), Gentian Violet (Humco)

## **Methods**

### *Sample Solution Preparation*

Hyaluronic acid solutions were prepared in 2 wt% concentrations in diH<sub>2</sub>O. Briefly, 2 wt% HA or 1.5 wt% HA + 0.5% TEMPO Cellulose fibers were added to warm diH<sub>2</sub>O in a conical tube. The solutions were vortexed before being placed on a vertical rotary device at 4°C overnight to ensure even hydration, dissolution, and dispersion of the polymers. The resulting viscous solutions were stored at 4°C until use.

### *Microneedle Fabrication*

Microneedles were fabricated by placing microneedle molds in 4mm deep acrylic wells specifically designed for the arrays. The molds were covered with approximately 500μL of a 2 wt% solution containing either 2 wt% hyaluronic acid or a composite containing HA or TEMPO-cellulose.

The molds were centrifuged at 3000 x G for 3 hours at 30°C to dry. The needles were dried in this fashion to mitigate curling. The molds were filled and dried for a total of 3 cycles. After the final cycle, the needles were filled with 1mL of solution and centrifuged at 1000rpm for 6 hours to create a backing layer.

The molds were then covered with 1mL of an EDC crosslinking solution. The solution contained 34.7mM EDC-HCl and 14.5mM NHS in 80% ethanol and was made fresh before

use. The microneedles were soaked in the solution overnight to ensure crosslinking. The needles were then dried in the centrifuge at 2000rpm for 3 hours.

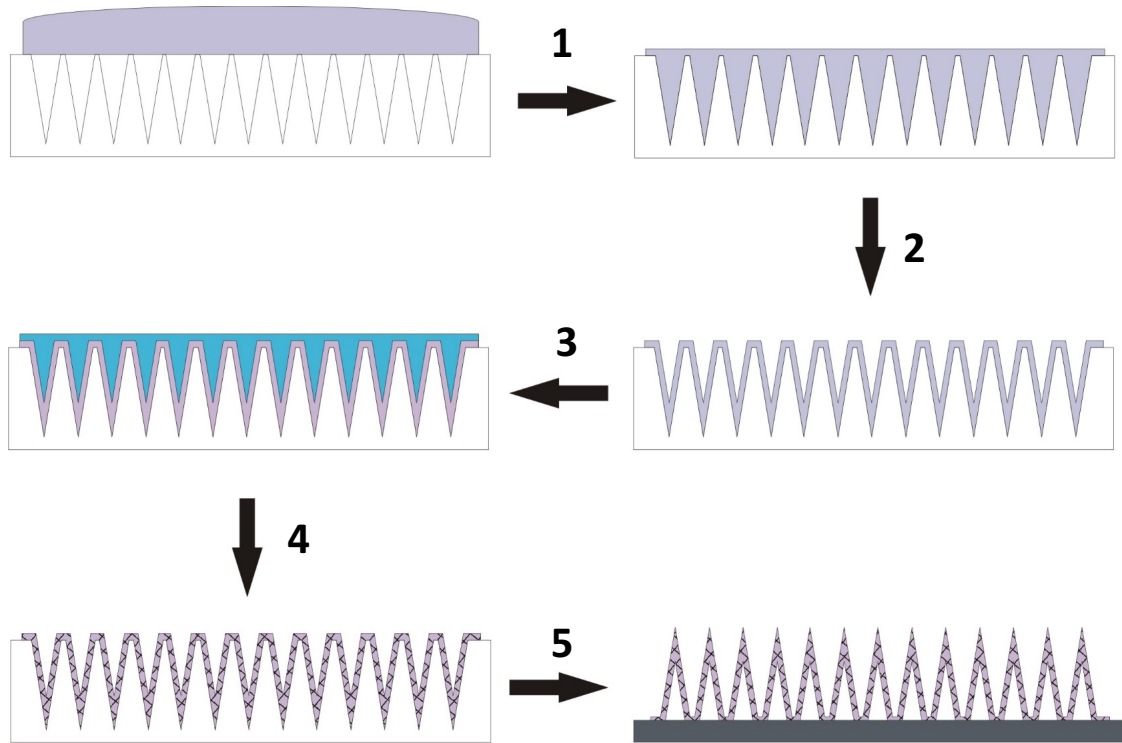


**Figure 21:** Schematic representation of the microneedle fabrication process. (1-2) loading and drying in centrifuge. (3) crosslinking. (4) drying. (5) removal from mold

### *Film Absorption*

Film absorption tests were performed by pipetting a desired test solution into each well of a 24-well culture plate. The solutions were dried under ambient conditions overnight in a desiccator.

Samples were prepared by pipetting 4 wt% of a HA or HA-cellulose composite or 2 wt% HA or 1.5 wt% HA + 0.5 wt% TEMPO cellulose 500 $\mu$ L into individual wells. Once dry,

the films were submerged in the crosslinking solution used to crosslink the microneedles. The samples were crosslinked overnight, then dried, rinsed with 1mL diH<sub>2</sub>O, then placed in a desiccator for two days to dry completely. The dry weights were recorded for each sample, then each sample was hydrated with diH<sub>2</sub>O for 3min. The hydrated films were touched to a Kimwipe for 1s on each side to remove excess water, then weighed. The mass difference was recorded as a percent change.

### *Needle Swelling*

Similar to the film absorption test, crosslinked microneedles fabricated of the same solutions were tested for three dimensional swelling. Briefly, microneedles were removed from molds by adhering them to a glass slide fitted with double-sided tape (3M). Single rows of needles were sectioned off from the array using a razor. The row was affixed to a clean slide, then placed on a goniometer platform under a pendent drop needle filled with diH<sub>2</sub>O.

The needle tip was adjusted such that the bore was filled with water, but none protruded from the needle tip. With the bore aligned with an individual needle, the platform was lifted to insert the needle into the bore. The needle was hydrated for 30s before the platform was lowered and the needle was imaged. Full-width-half-max comparisons were made between each sample for dry and wet microneedles to evaluate the swelling behavior of each polymer.

### *Fluid Wicking*

The ability of the microneedles to pull liquid from a surface and continuously transport it across an impermeable membrane is paramount to the success of this study. To demonstrate

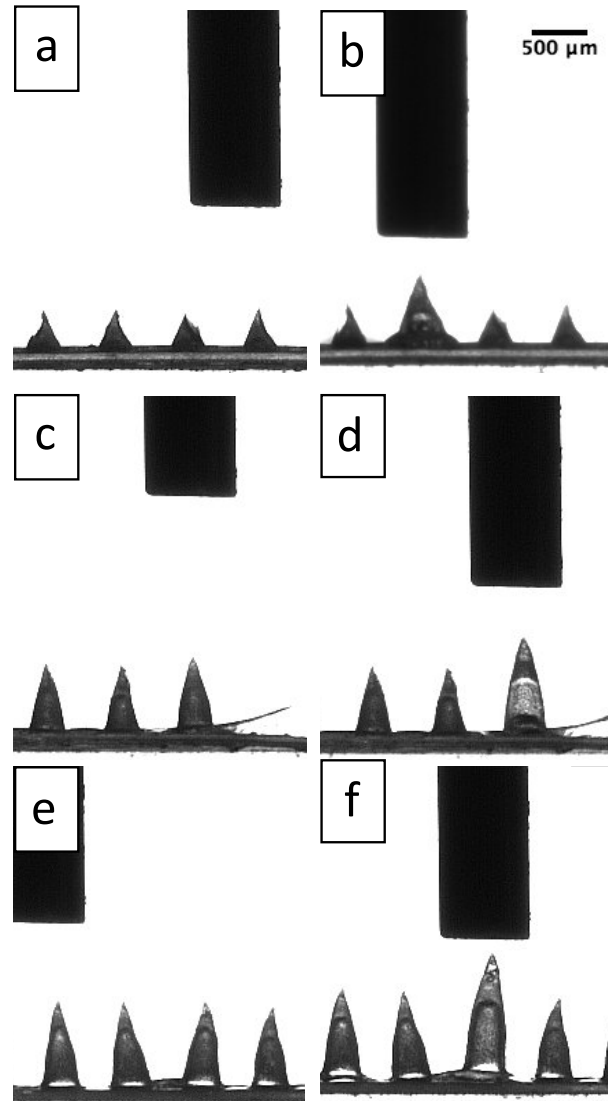


**Figure 22:** Full width half max experiment shows that crosslinked HA microneedles swell appreciably without deterioration. Dry 400, 600, & 800µm microneedles (a, c, & e, respectively) and wet 400, 600, & 800µm microneedles (b, d, & f, respectively).

this, microneedle arrays were mounted to a paper pump encased in laminating film. Briefly, a paper pump is a microfluidic device in which a piece of paper is cut to specific geometries. The pump has a sample inlet, a capillary transport region, a fluid sink, and a pressure

equilibration hole. The pump is driven entirely by capillary action. Aside from the inlet port and equilibration hole, the pump is sealed within an impermeable membrane to ensure fluid travels at a constant rate without evaporation.<sup>168</sup>

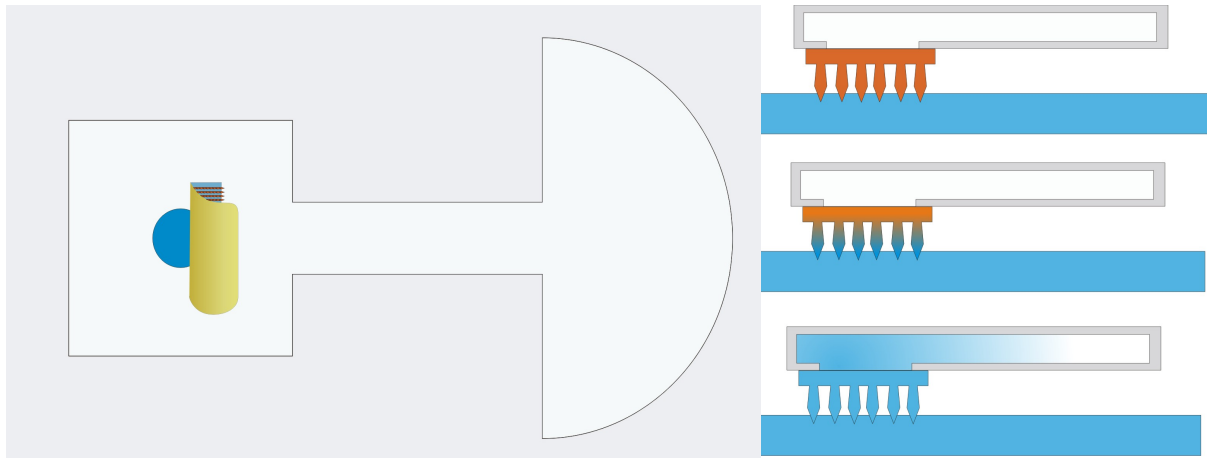


**Figure 23:** (Left) Schematic representation of the paper pump design used for wicking experiment. As can be seen, the microneedle array rests over the inlet hole. (Right) Side view schematic representation of fluid transport through the microneedles into the paper pump.

The assembled device was tested initially by soaking a piece of filter paper with dyed  $\text{dH}_2\text{O}$ , then gently resting the microneedle array on the filter paper. As the needles hydrated and swelled, they contacted the pump inlet port. Once in contact, the pump pulled the liquid at a constant rate, consistent with the wicking action observed by a paper pump.

### *Mechanical Characterization*

Crosslinked microneedles were cut into 3x1 arrays and placed on a mechanical compression device. The needles were compressed at a  $1 \mu\text{m}/\text{min}$  until completely compressed. The data was normalized such that all sample data initiated at a distance-force slope consistently greater than 0.1. The data was plotted as seen on **Table 2**.

*Puncture Testing:*

To assess whether HA microneedles were able to puncture skin, a skin mimic was developed from PDMS. The PDMS thin film was too robust and did not allow for puncturing but instead deformed around the needles.

To test whether the microneedles would puncture live tissue, a 3x5 microneedle array was adhered to a wooden substrate with cyanoacrylate glue. The mounted array was then sterilized in ethylene oxide before rapid application to alcohol swabbed skin, as recommended in the literature<sup>169</sup> The application area was then stained with Gentian Violet, a stain that is used to visualize puncture marks in the skin. The excess stain was removed with 70% Ethanol before being visualized under a dissecting microscope.

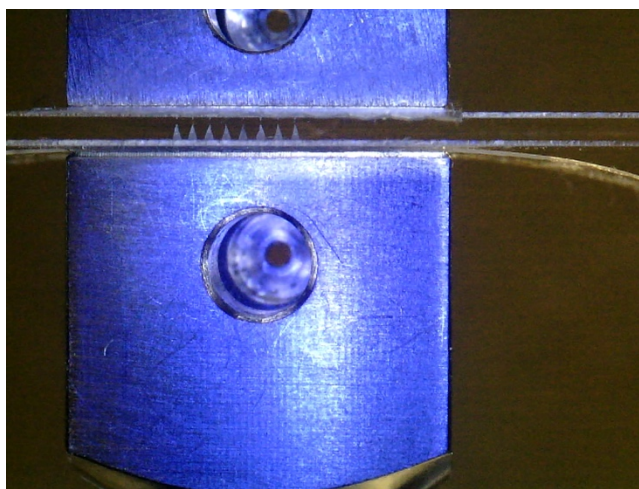


**Figure 24:** 600 $\mu$ m HA microneedles prior to compression testing.

## *Microbial Cellulose*

Cellulose incorporation is an integral aspect of this project. Microbial cellulose is of particular interest due to its ease of production and high mechanical properties. To get a background understanding of how this biopolymer interacts with other polymers, microbial cellulose was produced and analyzed according to standard laboratory protocols (**Appendix A**).

The physical properties of microbial cellulose are of interest for potential application as a wicking backing in later iterations of the project. The finer network of fibrils could lead to better fluid control in a paper-pump device.

## **Results & Discussion**

### *Film Absorption:*

Based on the film absorbance data, there are a few key observations. As the first step in the process for developing the crosslinked hydrogels, soaking and recovery of the films from deionized water demonstrates the effective crosslinking of hyaluronic acid. Furthermore, the crosslinked HA surrounds the TEMPO-cellulose microfibrils to efficiently create an interpenetrating network with enhanced wicking properties.

While fabricating and testing film absorbance, it was tested if increasing film solid content would provide better absorbance. As seen in **Figure 25**, addition of more solids lowers the water absorbing abilities of the hydrogel materials for both HA and HA composites. From

this experiment, it was deemed to be in the best interest to utilize 2 wt% solid solutions to cast all future microneedles.

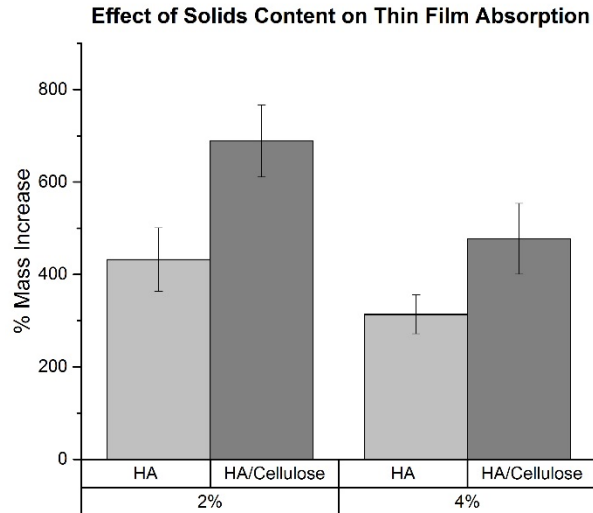


**Figure 25:** Comparison of 2 wt% and 4 wt% solids content films composed of either HA or a 50/50 blend of HA and Cellulose. Standard deviation calculated for each group: N=6

It can be seen in **Figure 26** that HA films absorb several times their weight in water. There is also a statistically significant (t-test) increase in the water absorption with added cellulose. This is due to the strong hydrogen bonding between water and cellulose and demonstrates the ability of cellulose to augment the absorptivity of HA-based thin films.

In the trials comparing the absorption between 500 $\mu$ L and 1500 $\mu$ L solutions, the difference between the unmodified HA and the HA-composite were not statistically significant. Comparing the 500 $\mu$ L 2% HA sample to the 1.5mL 2% HA sample yielded statistically different absorption values, whereas the 1.5% HA + 0.5% TEMPO composites did not show statistical difference. This leads to inconclusive evaluation as to whether the volume of material makes any difference in film absorption capacity.

The variation is likely due to the uncontrollable rolling of the hydrated films, which likely trapped water inside the barrel that formed as the needle arrays were submerged. Due to the

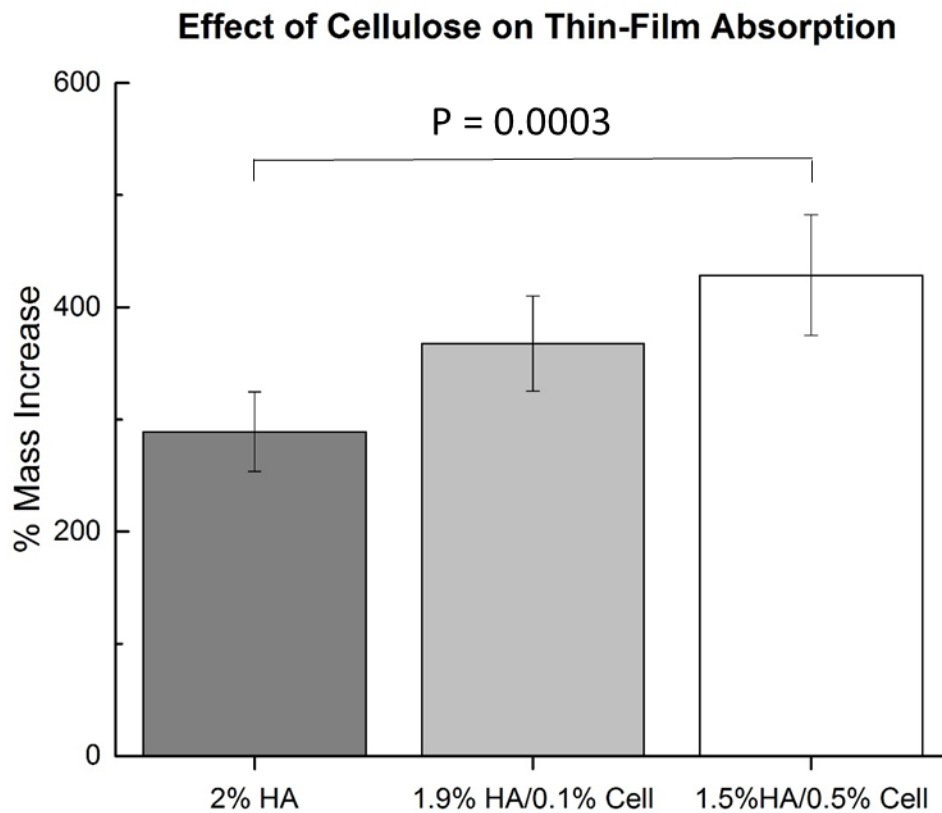


**Figure 26:** Mass increase across varying levels of cellulose in 2 wt% thin-film HA composites. Increasing cellulose content shows significant increase in absorption. Standard deviation calculated for each group: N=6

small scale, the trapped water could greatly alter the measured mass. It has been observed through the duration of these experiments that higher concentrations of polymer tend to curl towards the surface-air interface. This is a common effect seen in polymer science and is due to the increased contractile force at the liquid-air interface of the drying solution.

This phenomenon was mitigated using centrifugal drying for the microneedle arrays but was not possible for the thin film applications. Nevertheless, it is reasonable to assume from the thinner film deposition, which dried under less stress and yielded more uniform results, that the addition of TEMPO to a hyaluronic acid composite creates a more hydrophilic material than HA can provide alone.

### *Microneedle Fabrication*

The designed microneedle fabrication process proved to be challenging with the use of highly contracting biopolymers. High contractility is not a feature observed in many of the synthetic polymers used in the literature and was therefore not initially accounted for in the fabrication process. Despite the surprise, it could be somewhat counteracted with centrifugal force.

The needles produced with a centrifuge were mostly flat and uniform. One of the most interesting findings in this project was the natural formation and maintenance of hollow bore microneedles as can be seen in **Figure 27**. Because the needles are not crosslinked in solution, as many previous studies have done, the needles dry, constantly contracting towards the outside

wall of the mold. While unexpected, the result yields a more favorable product with even less fluid obstruction between the interstitium and the external wick.

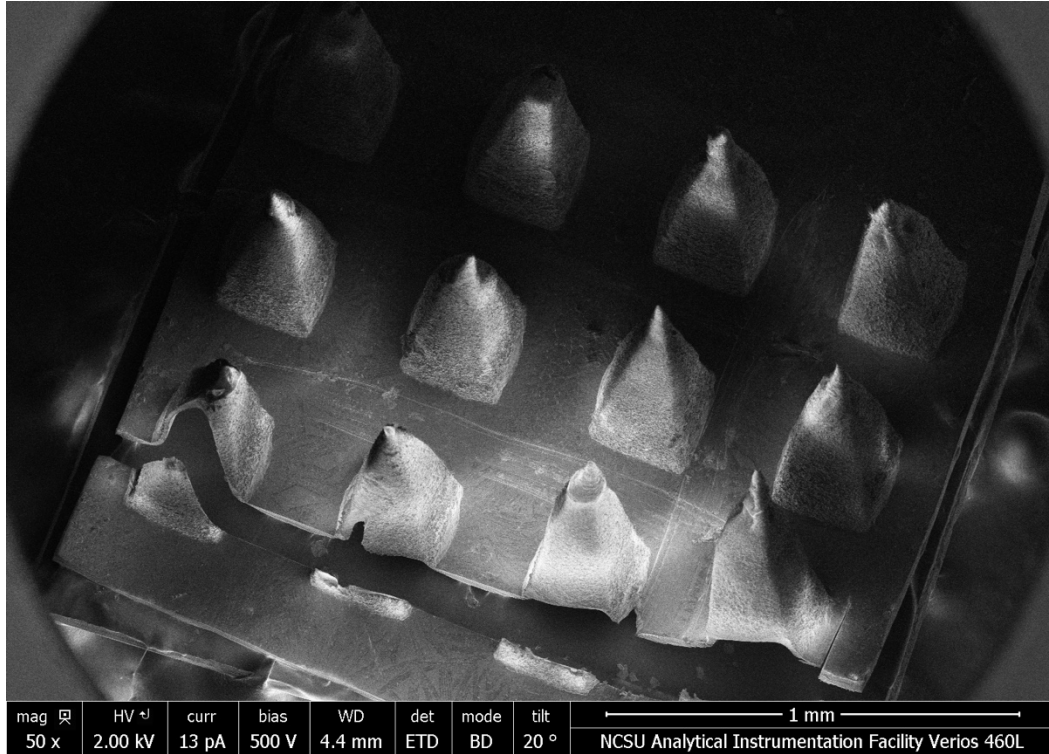


**Figure 27:** SEM image of 800 $\mu$ m HA microneedles displays defined square pyramidal geometry, while a horizontal incision shows hollow bodies

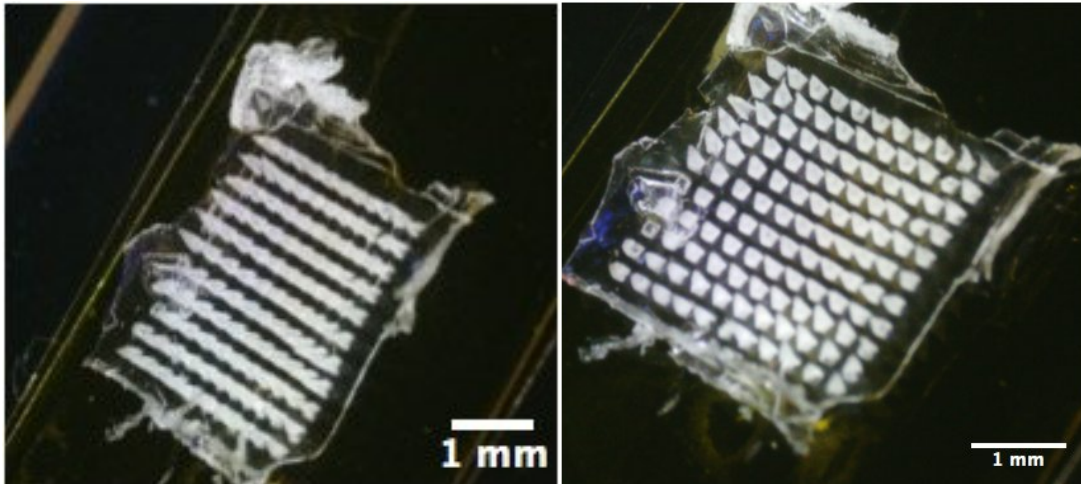


**Figure 28:** Microscope images of HA microneedles from the side (left) and from the top (right).

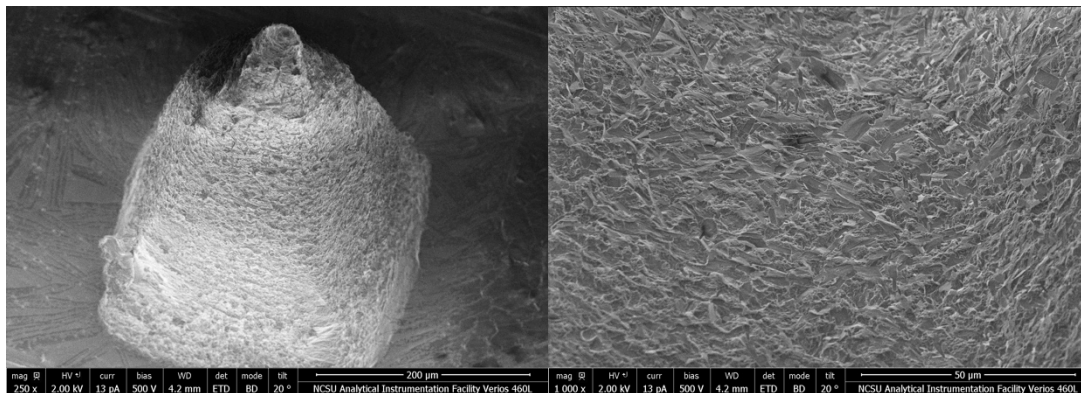


**Figure 29:** SEM image of HA microneedle with a high magnification of the fibrous network seen on the right.

### *Microneedle Swelling*

As seen in **Table 2** and **Figure 31**, both needle types swell similarly to approximately 26% of their original full width half max. Despite the similar swelling percentages, it is important to note the observational differences between the pure polymers and the composite materials.

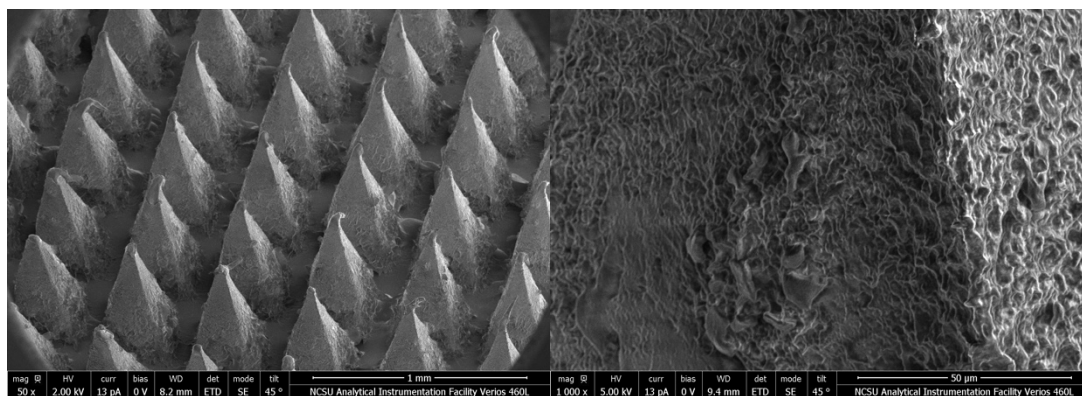


**Figure 30:** SEM image of Cellulose microneedles with a high magnification of the fibrous network seen on the right

**Table 2:** Average full width half max swelling increase data for microneedles. Calculated percent increase of dry vs wet microneedle. N=10 for each set.

### Full Width Half Max Increase

	2% HA	1.5% HA + 0.5% Cellulose
<b>400<math>\mu</math>m</b>	25.9%	27.9%
<b>600<math>\mu</math>m</b>	25.9%	29.9%
<b>800<math>\mu</math>m</b>	37.9%	27.1%

alone. Even more, cellulose does not dissolve in water as HA does. This leads to aggregate suspensions of cellulose fibers in solution. The heterogeneity of the solution increases as the needles dry, wherein cellulose aggregates dry and compact at a different rate than hyaluronic acid.

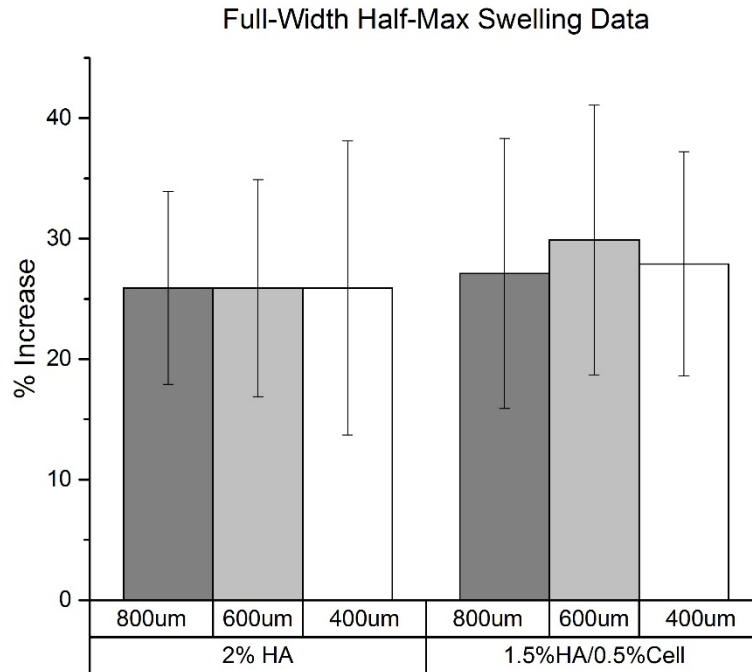


**Figure 31:** Full width half max swelling data shows little difference in volume change between HA and composite microneedles. Standard deviation calculated for each group: N=6

As cellulose dries, it forms tight intermolecular hydrogen bonding, much tighter than hyaluronic acid. This is because cellulose contains more hydrogen bonding sites per monomeric unit. Because of this feature, cellulose composites contract much more than HA

The effect of this can be seen across all samples of HA-cellulose composite and is a point of concern for continued development of the microneedle device. If the contraction cannot be controlled in such a way as to create more uniform needles, uniform devices cannot be realized.

*Microneedle Wicking*

Based on the results of the film and microneedle wicking experiments, the addition of cellulose to the thin films increases the overall water absorption but does not increase the ability of the material to swell. The combination of these data suggests that cellulose does indeed increase the hydrophilic nature of the microneedles. As mentioned before, increasing the hydrophilic nature of the microneedles is ultimately a step towards a wicking microneedle.

The design of this experiment was used to determine if the microneedle array could act as a conduit through which fluid could flow to a known wicking material. **Figure 32** shows that HA microneedles are able to act as passive conduits through which water can be wicked at a neutral, atmospheric pressure. The point at T0 shows an initial contacting of the microneedles with the pump. From that point, the fluid moves at a steady rate along the pump until the material is saturated. This experiment demonstrates the utility of paper pumps as passive pumping devices that absorb fluid at rates dependent on their shape. In this shape, five minutes was required to saturate the pump. These could be altered in such a way that enables

continuous extraction of ISF over longer periods of time however, making them suitable for long-term monitoring of analytes.

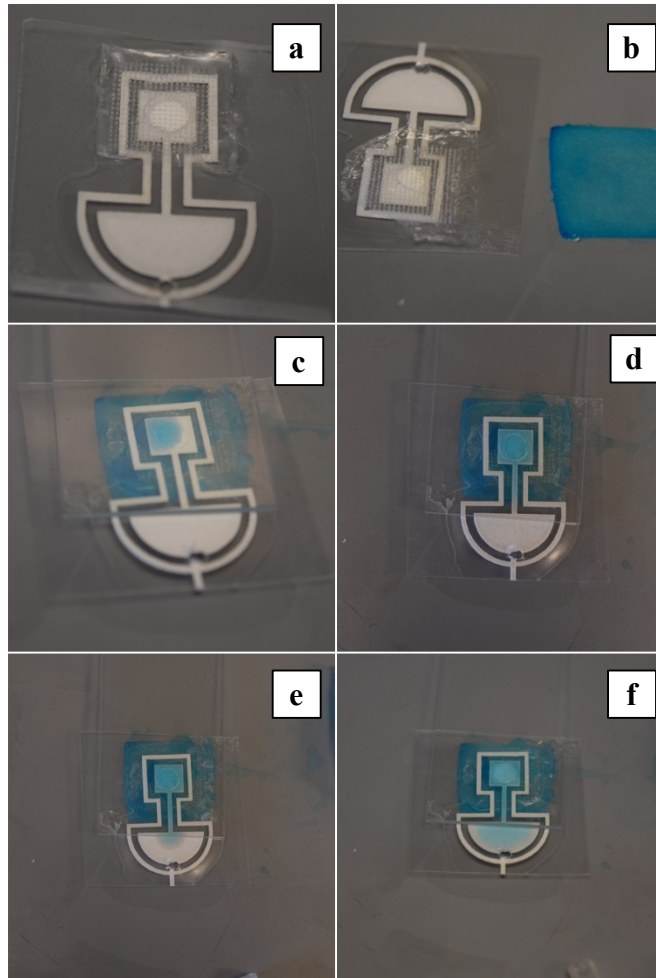
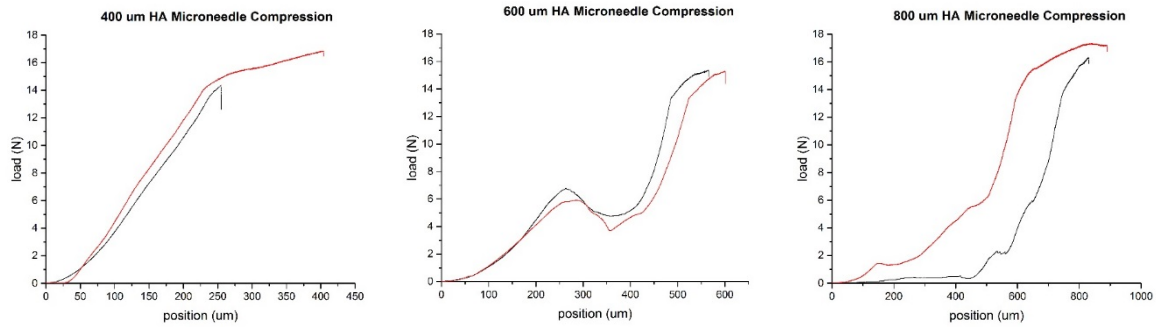


**Figure 32:** Assessment of fluid transport across impermeable membrane (a) Image of HA microneedle array attached to a microfluidic paper pump. (b) Setup blue dye on filter paper. (c, d, e, & f) Time points 0s, 40s, 80s, and 270s, respectively.

### *Microneedle Compression*

The ability for a microneedle array to puncture the skin is necessary for the realization of an interstitial fluid wicking device. **Figure 33** plots the results from HA microneedle

compression testing for 400, 600, & 800 $\mu$ m HA microneedles. Each graph shows the point at



### Mechanical Compression of HA Microneedles

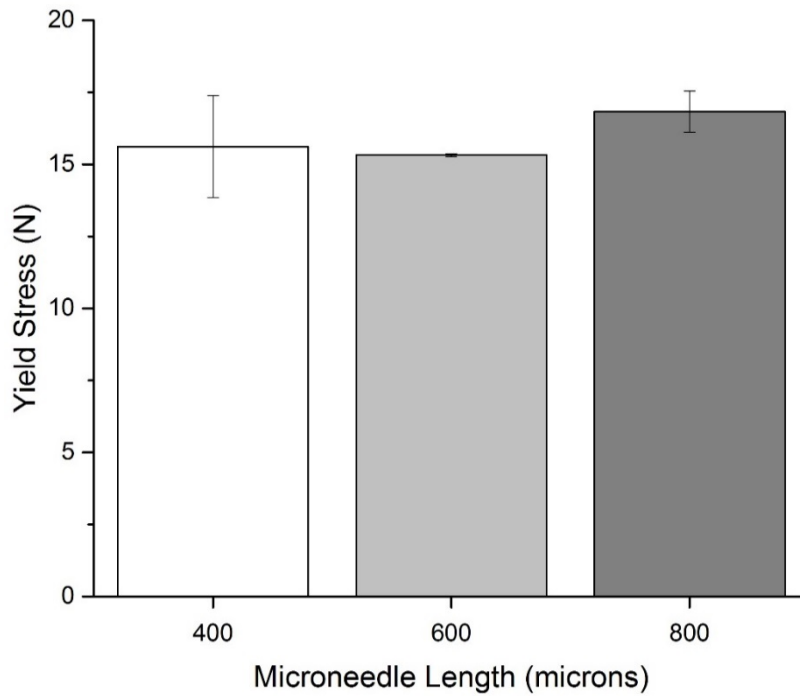
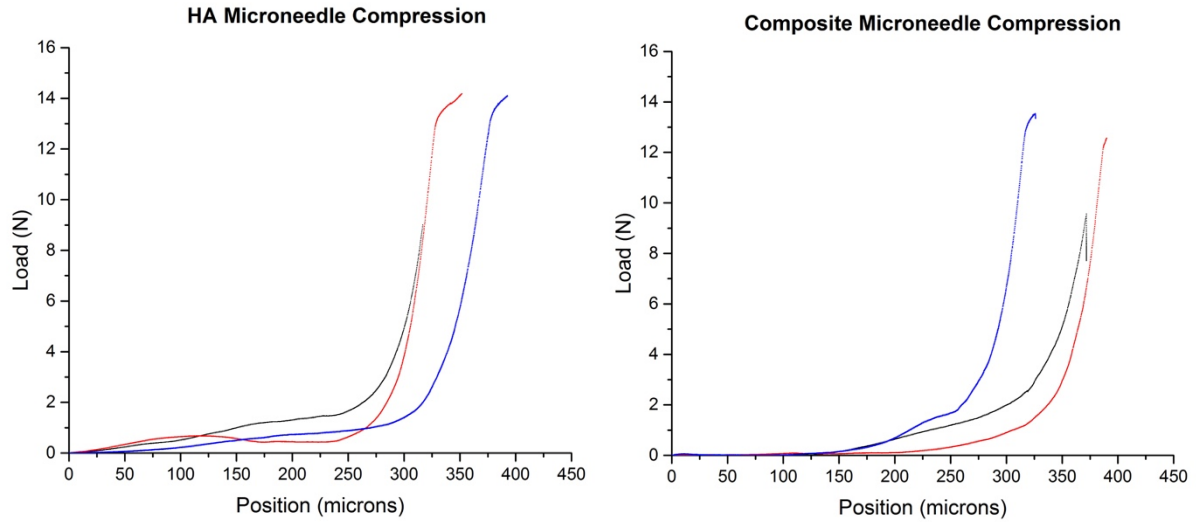


**Figure 33:** (top) Graphical data shows microneedle compression for individual samples of HA microneedles of varying lengths. (bottom) Bar chart displays average maxima for each data set. Standard deviation calculated for each group: N=2



### Microneedle Compression Test

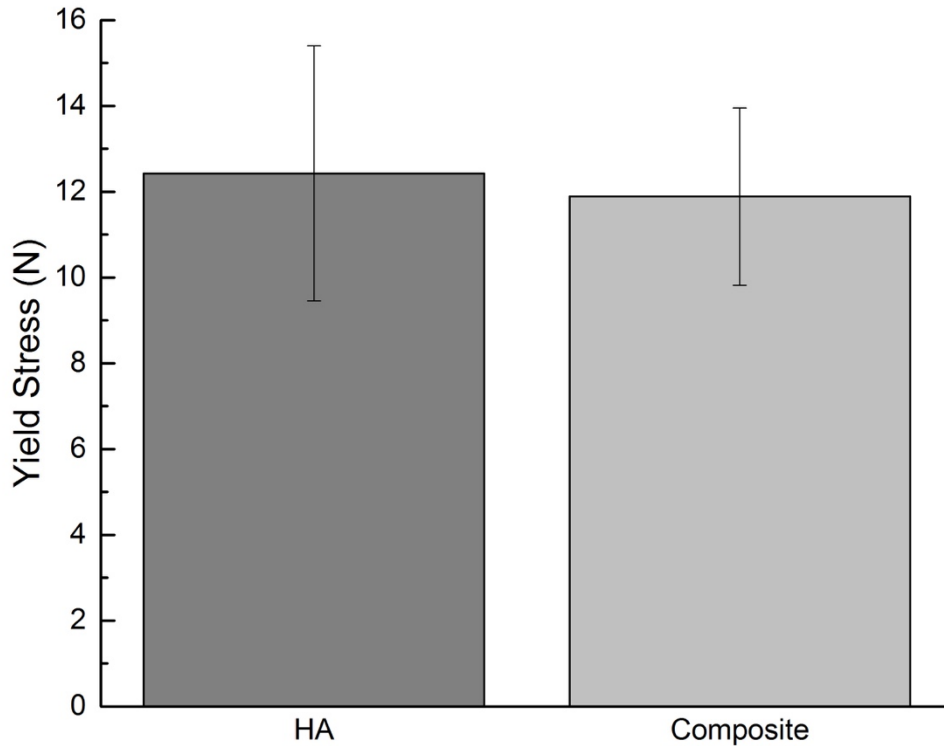


**Figure 34:** (top) Graphical data shows microneedle compression for individual samples of 600 $\mu$ m HA and HA Composite microneedles. (bottom) Bar chart displays average yield load for the above samples. Standard deviation calculated for each group: N=3

which the microneedles begin to break (~16N). This mark is above the 3N mark described

previously and exceeds the desired 10N threshold recommended in the literature.<sup>170</sup> Overcoming the theoretical barrier to skin puncture enabled further progress without changing the needle composition.

**Figure 34** compares the difference in compressive resistance between 600 $\mu$ m HA and HA Composite microneedles. There is a slight, but not statistically relevant, reduction in the resistance in the composite materials. As previously mentioned, reduction in mechanical integrity is likely a result of structural variance caused by non-uniform compaction during the drying process. Despite the slight reduction, it is promising that the variation is modest and could likely be remedied by using more uniform cellulose nanocrystals.

## **Conclusions & Future Directions**

As evidenced by the data, hyaluronic acid-TEMPO cellulose composites could be a viable material for microneedle-based continuous monitoring devices. The demonstrated ability of TEMPO cellulose to increase the water absorption capacity of hyaluronic acid without causing an increase in swelling indicates that there would be a rise in energy within the material and would enable the material to act as a wick in specific circumstances.

Attachment of a sink across a non-permeable membrane would provide the right set of circumstances to utilize the wicking properties developed within this project. It has been shown here that hyaluronic acid-based microneedles are suitable base materials for transporting a fluid from a source to a sink. Cellulose incorporation into the HA microneedles

has proven to increase the water affinity of the needles but has not been demonstrated against a negative pressure, as is seen in live interstitial fluid.

*Future Directions:*

The initial success of these biopolymer microneedles lays the foundation for future development of potentially useful and marketable products with ranging applications across health monitoring industries. Integration of sensors into fluid absorbing microneedle arrays could provide continuous data monitoring, which could enable better insight to a variety of areas of interest ranging from glucose monitoring, drug testing, athletic performance, or more.

This work has provided the basis for development of biomaterial-based hydrogel microneedles with the rigidity needed to pierce the stratum corneum and the ability to transport fluid across impermeable membranes. Moving forward, this technology can be built upon by incorporating new paper pump designs to extend the wicking time for the device and by experimenting with new polymer blends to increase water affinity and mechanical integrity.

Optical sensors are a proposed method used to analyze ISF contents for self-contained wearable sensing platforms. Using reflective IR, passive pumps can be outfitted with a small sensor array at the microneedle port to detect analytes of interest in real time. Such sensors can be tuned to detect a wide range of molecules, or even used in tandem to detect specific markers of health or disease.

Additionally, the proposed use of paper pumps can be built upon by utilizing microbial cellulose. Microbial cellulose is made of longer, more entangled fibers, which add to the mechanical properties. Microbial cellulose, when dried, forms a very thin and dense fiber

network. The thinness lends itself to long-term use as thin materials conform to the skin. Long fiber networks enable the thin material to bend without breaking or forming permanent bends, which could alter fluid flow. Furthermore, the density of a fiber network can be manipulated to adjust wicking rates based on desired application.

This work has provided a strong foundation for a wide variety of applications for biomaterial-based wicking sensors. With continued research, this technology could open a cost effective path towards disposable health monitoring systems that provide continuous feedback. Safe, convenient, continuous data monitoring could provide great insight to disease states and progression, as well as a wide variety of other health information for the quantified self.

## REFERENCES

- 1 Cole, L. & Kramer, P. R., - (2016).
- 2 Pickup, J. Sensitive glucose sensing in diabetes. *The Lancet* **355**, 426-427 (2000).
- 3 Guyton, A. C., Granger, H. J. & Taylor, A. E. Interstitial Fluid Pressure. *Physiological Reviews* **51**, 527-& (1971).
- 4 Kim, Y. C., Park, J. H. & Prausnitz, M. R. Microneedles for drug and vaccine delivery. *Advanced Drug Delivery Reviews* **64**, 1547-1568, doi:10.1016/j.addr.2012.04.005 (2012).
- 5 Polat, B. E., Hart, D., Langer, R. & Blankschtein, D. Ultrasound-mediated transdermal drug delivery: Mechanisms, scope, and emerging trends. *J Control Release* **152**, 330-348, doi:10.1016/j.jconrel.2011.01.006 (2011).
- 6 Boucher, Y., Kirkwood, J. M., Opacic, D., Desantis, M. & Jain, R. K. Interstitial Hypertension in Superficial Metastatic Melanomas in Humans. *Cancer Research* **51**, 6691-6694 (1991).
- 7 Elmquist, W. F. Application of Microdialysis in Pharmacokinetic Studies. *Pharmaceutical Research* **14**, 21, doi:10.1023/A:1012081501464 (1997).
- 8 Costanzo, U., Streit, M. & Braathen, L. R. Autologous suction blister grafting for chronic leg ulcers. *Journal of the European Academy of Dermatology and Venereology* **22**, 7-10, doi:10.1111/j.1468-3083.2007.02148.x (2008).
- 9 Mitragotri, S., Coleman, M., Kost, J. & Langer, R. Transdermal extraction of analytes using low-frequency ultrasound. *Pharmaceutical Research* **17**, 466-470, doi:10.1023/A:1007537222591 (2000).
- 10 Donnelly, R. F. *et al.* Hydrogel-Forming Microneedles Prepared from "Super Swelling" Polymers Combined with Lyophilised Wafers for Transdermal Drug Delivery. *Plos One* **9**, doi:10.1371/journal.pone.0111547 (2014).
- 11 Aigner, B. A. *et al.* Dermal open-flow microperfusion as a novel technique for in vivo measurement of dermal interstitium. *Experimental Dermatology* **21**, e13-e13 (2012).
- 12 Donnelly, R. F. *et al.* Hydrogel-Forming Microneedle Arrays for Enhanced Transdermal Drug Delivery. *Advanced Functional Materials* **22**, 4879-4890, doi:10.1002/adfm.201200864 (2012).
- 13 Swan, M. THE QUANTIFIED SELF: Fundamental Disruption in Big Data Science and Biological Discovery. *Big Data* **1**, 85-99, doi:10.1089/big.2012.0002 (2013).
- 14 Alavi, A. H., Hasni, H., Lajnef, N. & Chatti, K. Continuous health monitoring of pavement systems using smart sensing technology. *Construction and Building Materials* **114**, 719-736, doi:10.1016/j.conbuildmat.2016.03.128 (2016).
- 15 Balouchestani, M., Raahemifar, K. & Krishnan, S. in *2012 Ieee 55th International Midwest Symposium on Circuits and Systems Midwest Symposium on Circuits and Systems Conference Proceedings* (eds A. Garimella & C. C. Purdy) 916-919 (2012).
- 16 Jara, A. J., Silva, R. M., Silva, J. S., Zamora, M. A. & Skarmeta, A. F. G. Mobile IP-Based Protocol for Wireless Personal Area Networks in Critical Environments.

- Wireless Personal Communications* **61**, 711-737, doi:10.1007/s11277-011-0428-y (2011).
- 17 Jung, S., Ji, T. & Varadan, V. K. Point-of-care temperature and respiration monitoring sensors for smart fabric applications. *Smart Materials & Structures* **15**, 1872-1876, doi:10.1088/0964-1726/15/6/042 (2006).
- 18 Neild, I., Heatley, D. J. T., Kalawsky, R. S. & Bowman, P. A. Sensor networks for continuous health monitoring. *Bt Technology Journal* **22**, 130-139, doi:10.1023/b:bttj.0000047127.01462.49 (2004).
- 19 Pasche, S. *et al.* in *Biomedical Applications of Smart Materials, Nanotechnology and Micro/Nano Engineering Vol. 57 Advances in Science and Technology* (eds P. Vincenzini & D. DeRossi) 80-87 (2009).
- 20 Tee, B. C. K. *et al.* Tunable Flexible Pressure Sensors using Microstructured Elastomer Geometries for Intuitive Electronics. *Advanced Functional Materials* **24**, 5427-5434, doi:10.1002/adfm.201400712 (2014).
- 21 Xiao, S., Dharndhere, A., Sivaraman, V. & Burdett, A. Transmission Power Control in Body Area Sensor Networks for Healthcare Monitoring. *Ieee Journal on Selected Areas in Communications* **27**, 37-48, doi:10.1109/jsac.2009.090105 (2009).
- 22 Yoo, J., Yan, L., Lee, S., Kim, Y. & Yoo, H. J. A 5.2 mW Self-Configured Wearable Body Sensor Network Controller and a 12  $\mu$ W Wirelessly Powered Sensor for a Continuous Health Monitoring System. *Ieee Journal of Solid-State Circuits* **45**, 178-188, doi:10.1109/jssc.2009.2034440 (2010).
- 23 Murray, E. C., Deighan, C., Geddes, C. & Thomson, P. C. Taurolidine-citrate-heparin catheter lock solution reduces staphylococcal bacteraemia rates in haemodialysis patients. *Qjm-an International Journal of Medicine* **107**, 995-1000, doi:10.1093/qjmed/hcu128 (2014).
- 24 Koschinsky, T. & Heinemann, L. Sensors for glucose monitoring: technical and clinical aspects. *Diabetes-Metabolism Research and Reviews* **17**, 113-123, doi:10.1002/dmrr.188 (2001).
- 25 Wilinska, M. E. *et al.* Interstitial glucose kinetics in subjects with type 1 diabetes under physiologic conditions. *Metabolism-Clinical and Experimental* **53**, 1484-1491, doi:10.1016/j.metabol.2004.05.014 (2004).
- 26 Yu, H. X., Li, D. C., Roberts, R. C., Xu, K. X. & Tien, N. C. An Interstitial Fluid Transdermal Extraction System for Continuous Glucose Monitoring. *Journal of Microelectromechanical Systems* **21**, 917-925, doi:10.1109/JMEMS.2012.2192910 (2012).
- 27 Zimmerli, W., Sansano, S. & Wittke, B. Pharmacokinetics of cefetamet in plasma and skin blister fluid. *Antimicrobial Agents and Chemotherapy* **40**, 102-104 (1996).
- 28 Foghandersen, N., Altura, B. M., Altura, B. T. & Siggaardandersen, O. COMPOSITION OF INTERSTITIAL FLUID. *Clinical Chemistry* **41**, 1522-1525 (1995).
- 29 Levick, J. R. & Michel, C. C. Microvascular fluid exchange and the revised Starling principle. *Cardiovascular Research* **87**, 198-210, doi:10.1093/cvr/cvq062 (2010).

- 30 Liu, X. R. *et al.* Unbound Drug Concentration in Brain Homogenate and Cerebral Spinal Fluid at Steady State as a Surrogate for Unbound Concentration in Brain Interstitial Fluid. *Drug Metabolism and Disposition* **37**, 787-793, doi:10.1124/dmd.108.024125 (2009).
- 31 Nishiyama, A., Seth, D. M. & Navar, L. G. Renal interstitial fluid concentrations of angiotensins I and II in anesthetized rats. *Hypertension* **39**, 129-134, doi:10.1161/hy0102.100536 (2002).
- 32 Poulin, P. & Theil, F. P. A Priori prediction of tissue : plasma partition coefficients of drugs to facilitate the use of physiologically-based pharmacokinetic models in drug discovery. *Journal of Pharmaceutical Sciences* **89**, 16-35, doi:10.1002/(sici)1520-6017(200001)89:1<16::aid-jps3>3.0.co;2-e (2000).
- 33 Sjostrand, M. *et al.* Delayed transcapillary transport of insulin to muscle interstitial fluid in obese subjects. *Diabetes* **51**, 2742-2748, doi:10.2337/diabetes.51.9.2742 (2002).
- 34 Haslene-Hox, H. *et al.* A New Method for Isolation of Interstitial Fluid from Human Solid Tumors Applied to Proteomic Analysis of Ovarian Carcinoma Tissue. *Plos One* **6**, doi:10.1371/journal.pone.0019217 (2011).
- 35 Ledger, P. W. Skin Biological Issues in Electrically Enhanced Transdermal Delivery. *Advanced Drug Delivery Reviews* **9**, 289-307, doi:10.1016/0169-409X(92)90027-N (1992).
- 36 Proksch, E., Brandner, J. M. & Jensen, J. M. The skin: an indispensable barrier. *Experimental Dermatology* **17**, 1063-1072, doi:10.1111/j.1600-0625.2008.00786.x (2008).
- 37 Wiig, H. & Swartz, M. A. Interstitial Fluid and Lymph Formation and Transport: Physiological Regulation and Roles in Inflammation and Cancer. *Physiological Reviews* **92**, 1005-1060, doi:10.1152/physrev.00037.2011 (2012).
- 38 Zimmerman, A., Bai, L. & Ginty, D. D. The gentle touch receptors of mammalian skin. *Science* **346**, 950-954, doi:10.1126/science.1254229 (2014).
- 39 Brouns, F. *et al.* Glycaemic index methodology. *Nutrition Research Reviews* **18**, 145-171, doi:10.1079/nrr2005100 (2005).
- 40 Daffos, F., Capellapavlovsky, M. & Forestier, F. FETAL BLOOD-SAMPLING DURING PREGNANCY WITH USE OF A NEEDLE GUIDED BY ULTRASOUND - A STUDY OF 606 CONSECUTIVE CASES. *American Journal of Obstetrics and Gynecology* **153**, 655-660 (1985).
- 41 Solovey, A. *et al.* Circulating activated endothelial cells in sickle cell anemia. *New Engl J Med* **337**, 1584-1590, doi:10.1056/nejm199711273372203 (1997).
- 42 Taheri, S., Lin, L., Austin, D., Young, T. & Mignot, E. Short sleep duration is associated with reduced leptin, elevated ghrelin, and increased body mass index. *Plos Medicine* **1**, 210-217, doi:10.1371/journal.pmed.0010062 (2004).
- 43 Vincent, J. L. *et al.* Anemia and blood transfusion in critically ill patients. *Jama-Journal of the American Medical Association* **288**, 1499-1507, doi:10.1001/jama.288.12.1499 (2002).

- 44 Aspelund, A. *et al.* A dural lymphatic vascular system that drains brain interstitial fluid and macromolecules. *Journal of Experimental Medicine* **212**, 991-999, doi:10.1084/jem.20142290 (2015).
- 45 Gross, P. M. MORPHOLOGY AND PHYSIOLOGY OF CAPILLARY SYSTEMS IN SUBREGIONS OF THE SUBFORNICAL ORGAN AND AREA POSTREMA. *Canadian Journal of Physiology and Pharmacology* **69**, 1010-1025 (1991).
- 46 Sakka, L., Coll, G. & Chazal, J. Anatomy and physiology of cerebrospinal fluid. *European Annals of Otorhinolaryngology-Head and Neck Diseases* **128**, 309-316, doi:10.1016/j.anorl.2011.03.002 (2011).
- 47 Swartz, M. A. The physiology of the lymphatic system. *Advanced Drug Delivery Reviews* **50**, 3-20, doi:10.1016/s0169-409x(01)00150-8 (2001).
- 48 Xu, S. *et al.* INSULIN-LIKE GROWTH-FACTORS (IGFS) AND IGF-BINDING PROTEINS IN HUMAN SKIN INTERSTITIAL FLUID. *Journal of Clinical Endocrinology & Metabolism* **80**, 2940-2945, doi:10.1210/jc.80.10.2940 (1995).
- 49 Jamada, K. & Jodlbauer, A. The resorption means of the skin for aniline pigments with and without application of electrical currents (Iontophoresis) and iontophoresis in general. *Archives Internationales De Pharmacodynamie Et De Therapie* **19**, 215-228 (1909).
- 50 Kramer, D. W. The use of acetyl-beta-methylcholine chloride by iontophoresis in peripheral vascular diseases. *American Journal of the Medical Sciences* **193**, 405-413, doi:10.1097/00000441-193719330-00011 (1937).
- 51 Erlanger, G. Effect of iontophoresis in eye complaints. Successful lightening of the maculae cornea. *Deutsche Medizinische Wochenschrift* **46**, 1107-1109 (1920).
- 52 Benjamin, F. B. & Helvey, W. M. Iontophoresis of Potassium for Experimental Determination of Pain Endurance in Man. *Proceedings of the Society for Experimental Biology and Medicine* **113**, 566-& (1963).
- 53 Popkin, R. J. Penicillin by Iontophoresis. *Jama-Journal of the American Medical Association* **132**, 238-238 (1946).
- 54 Witzel, S. H., Fielding, I. Z. & Ormsby, H. L. Ocular Penetration of Antibiotics by Iontophoresis. *American Journal of Ophthalmology* **42**, 89-95 (1956).
- 55 Szabadi, E. & Bradshaw, C. M. Spread of Drugs in Tissue - Diffusion or Iontophoresis. *Journal of Theoretical Biology* **42**, 185-187, doi:10.1016/0022-5193(73)90158-6 (1973).
- 56 Gangarosa, L. P., Haynes, M. & Mahan, P. E. Iontophoresis of Drugs for Therapy of Postherpetic Neuralgia. *Proceedings of the Society for Experimental Biology and Medicine* **172**, 133-133 (1983).
- 57 Sloan, J. B. & Soltani, K. Iontophoresis in Dermatology. *Journal of the American Academy of Dermatology* **15**, 671-684, doi:10.1016/S0190-9622(86)70223-5 (1986).
- 58 Behar-Cohen, F. *et al.* Iontophoresis: past and future. *Journal Francais D Ophtalmologie* **24**, 319-327 (2001).
- 59 Nair, A. B. *et al.* Ungual and Trans-Ungual Iontophoretic Delivery of Terbinafine for the Treatment of Onychomycosis. *Journal of Pharmaceutical Sciences* **98**, 4130-4140, doi:10.1002/jps.21711 (2009).

- 60 Goldstein, J. *et al.* A Sumatriptan Iontophoretic Transdermal System for the Acute Treatment of Migraine. *Headache* **52**, 1402-1410, doi:10.1111/j.1526-4610.2012.02198.x (2012).
- 61 Wu, X. M., Todo, H. & Sugibayashi, K. Enhancement of skin permeation of high molecular compounds by a combination of microneedle pretreatment and iontophoresis. *J Control Release* **118**, 189-195, doi:10.1016/j.jconrel.2006.12.017 (2007).
- 62 Chen, H. B. *et al.* Iontophoresis-driven penetration of nanovesicles through microneedle-induced skin microchannels for enhancing transdermal delivery of insulin. *J Control Release* **139**, 63-72, doi:10.1016/j.jconrel.2009.05.031 (2009).
- 63 Lanke, S. S. S., Kolli, C. S., Strom, J. G. & Banga, A. K. Enhanced transdermal delivery of low molecular weight heparin by barrier perturbation. *International Journal of Pharmaceutics* **365**, 26-33, doi:10.1016/j.ijpharm.2008.08.028 (2009).
- 64 Kigasawa, K. *et al.* Noninvasive delivery of siRNA into the epidermis by iontophoresis using an atopic dermatitis-like model rat. *International Journal of Pharmaceutics* **383**, 157-160, doi:10.1016/j.ijpharm.2009.08.036 (2010).
- 65 Tomoda, K. *et al.* Enhanced transdermal delivery of indomethacin-loaded PLGA nanoparticles by iontophoresis. *Colloids and Surfaces B-Biointerfaces* **88**, 706-710, doi:10.1016/j.colsurfb.2011.08.004 (2011).
- 66 Nixon, S., Sieg, A., Delgado-Charro, M. B. & Guy, R. H. Reverse iontophoresis of L-lactate: In vitro and in vivo studies. *Journal of Pharmaceutical Sciences* **96**, 3457-3465, doi:10.1002/jps.20989 (2007).
- 67 Wascotte, V. *et al.* Monitoring of urea and potassium by reverse iontophoresis in vitro. *Pharmaceutical Research* **24**, 1131-1137, doi:10.1007/s11095-007-9237-0 (2007).
- 68 Ching, C. T. S. & Connolly, P. Reverse iontophoresis: A non-invasive technique for measuring blood lactate level. *Sensors and Actuators B-Chemical* **129**, 352-358, doi:10.1016/j.snb.2007.08.031 (2008).
- 69 Lee, C. K. *et al.* Non-invasive and transdermal measurement of blood uric acid level in human by electroporation and reverse iontophoresis. *International Journal of Nanomedicine* **5**, 991-997, doi:10.2147/IJN.S14284 (2010).
- 70 McCormick, C., Heath, D. & Connolly, P. Towards blood free measurement of glucose and potassium in humans using reverse iontophoresis. *Sensors and Actuators B-Chemical* **166**, 593-600, doi:10.1016/j.snb.2012.03.016 (2012).
- 71 Bikbova, G. & Bikbov, M. Transepithelial corneal collagen cross-linking by iontophoresis of riboflavin. *Acta Ophthalmologica* **92**, E30-E34, doi:10.1111/aos.12235 (2014).
- 72 Leboulanger, B., Aubry, J. M., Bondolfi, G., Guy, R. H. & Delgado-Charro, M. B. Lithium monitoring by reverse iontophoresis in vivo. *Clinical Chemistry* **50**, 2091-2100, doi:10.1373/clinchem.2004.034249 (2004).
- 73 Inc, C. (2002).
- 74 Mastropasqua, L. *et al.* Corneal Cross-linking: Intrastromal Riboflavin Concentration in Iontophoresis-Assisted Imbibition Versus Traditional and Transepithelial

- Techniques. *American Journal of Ophthalmology* **157**, 623-630, doi:10.1016/j.ajo.2013.11.018 (2014).
- 75 Donnelly, R. F. *et al.* Microneedle-Mediated Minimally Invasive Patient Monitoring. *Therapeutic Drug Monitoring* **36**, 10-17 (2014).
- 76 Caffarel-Salvador, E. *et al.* Hydrogel-Forming Microneedle Arrays Allow Detection of Drugs and Glucose In Vivo: Potential for Use in Diagnosis and Therapeutic Drug Monitoring. *Plos One* **10**, doi:10.1371/journal.pone.0145644 (2015).
- 77 Hussein, G. A., de la Rosa, M. A. D., Richardson, E. S., Christensen, D. A. & Pitt, W. G. The role of cavitation in acoustically activated drug delivery. *J Control Release* **107**, 253-261, doi:10.1016/j.jconrel.2005.06.015 (2005).
- 78 Mitragotri, S., Edwards, D. A., Blankschtein, D. & Langer, R. Mechanistic Study of Ultrasonically-Enhanced Transdermal Drug-Delivery. *Journal of Pharmaceutical Sciences* **84**, 697-706, doi:10.1002/jps.2600840607 (1995).
- 79 Mitragotri, S., Blankschtein, D. & Langer, R. Transdermal drug delivery using low-frequency sonophoresis. *Pharmaceutical Research* **13**, 411-420, doi:10.1023/A:1016096626810 (1996).
- 80 Alexander, A. *et al.* Approaches for breaking the barriers of drug permeation through transdermal drug delivery. *J Control Release* **164**, 26-40, doi:10.1016/j.jconrel.2012.09.017 (2012).
- 81 Mitragotri, S. & Kost, J. Low frequency sonophoresis: A noninvasive method of drug delivery and diagnostics. *Biotechnology Progress* **16**, 488-492, doi:10.1021/bp000024+ (2000).
- 82 Mitragotri, S., Coleman, M., Kost, J. & Langer, R. Analysis of ultrasonically extracted interstitial fluid as a predictor of blood glucose levels. *Journal of Applied Physiology* **89**, 961-966 (2000).
- 83 Zarshenas, M. M. Hajamat in Traditional Persian Medicine. *Journal of Evidence-Based Complementary & Alternative Medicine* **19** (2014).
- 84 Carlotti, P. in *Men's Health* (2016).
- 85 Bruun, J. N., Bredesen, J. E., Kierulf, P. & Lunde, P. K. M. Pharmacokinetic Studies of Antibacterial Agents Using the Suction Blister Method. *Scandinavian Journal of Infectious Diseases*, 49-53 (1991).
- 86 Vaillant, L., Autret, E., Marchand, S., Lorette, G. & Grenier, B. Suction Blisters Technique in Amikacin Diffusion through Interstitial Fluid in Cystic-Fibrosis. *Developmental Pharmacology and Therapeutics* **16**, 29-32 (1991).
- 87 Mazzei, T. *et al.* Penetration of Cefotetan into Suction Skin Blister Fluid and Tissue-Homogenates in Patients Undergoing Abdominal-Surgery. *Antimicrobial Agents and Chemotherapy* **38**, 2221-2223 (1994).
- 88 Sjolinforsberg, G., Berne, B., Blixt, C., Johansson, M. & Lindstrom, B. Chloroquine Phosphate - a Long-Term Follow-up of Drug Concentrations in Skin Suction Blister Fluid and Plasma. *Acta Dermato-Venereologica* **73**, 426-429 (1993).
- 89 Walker, J. S., Knihinicki, R. D., Seideman, P. & Day, R. O. Pharmacokinetics of Ibuprofen Enantiomers in Plasma and Suction Blister Fluid in Healthy-Volunteers.

- Journal of Pharmaceutical Sciences* **82**, 787-790, doi:10.1002/jps.2600820806 (1993).
- 90 Williams, K. M., Pallapies, D., Peskar, B. A., Brune, K. & Geisslinger, G. The Suction Blister - a Human-Model to Study the Pharmacokinetics and Pharmacodynamics of Nsaids. *Clinical Pharmacology & Therapeutics* **57**, 159-159 (1995).
- 91 Ameglio, F., Bonifati, C., Pietravalle, M. & Fazio, M. Interleukin-6 and Tumor-Necrosis-Factor Levels Decrease in the Suction Blister Fluids of Psoriatic Patients during Effective Therapy. *Dermatology* **189**, 359-363 (1994).
- 92 Corstjens, H., Oikarinen, A., Richard, M. J., Declercq, L. & Maes, D. Positive correlation between catalase activity and collagen synthesis in suction blister fluid. *Journal of Investigative Dermatology* **117**, 795-795 (2001).
- 93 Sun, C. C., Wu, J., Wong, T. T., Wang, L. F. & Chuan, M. T. High levels of interleukin-8, soluble CD4 and soluble CD8 in bullous pemphigoid blister fluid. The relationship between local cytokine production and lesional T-cell activities. *British Journal of Dermatology* **143**, 1235-1240, doi:10.1046/j.1365-2133.2000.03894.x (2000).
- 94 Brockow, K. *et al.* Levels of mast-cell growth factors in plasma and in suction skin blister fluid in adults with mastocytosis: Correlation with dermal mast-cell numbers and mast-cell tryptase. *Journal of Allergy and Clinical Immunology* **109**, 82-88, doi:10.1067/mai.2001.120524 (2002).
- 95 Dragatin, C. *et al.* Secukinumab distributes into dermal interstitial fluid of psoriasis patients as demonstrated by open flow microperfusion. *Experimental Dermatology* **25**, 157-159, doi:10.1111/exd.12863 (2016).
- 96 Gerritsen, R., Lutterman, J. A. & Jansen, J. A. A percutaneous device to study glucose kinetics in subcutaneous tissue fluid. *Journal of Materials Science-Materials in Medicine* **11**, 499-503 (2000).
- 97 Fischer, U., Ertle, R., Rebrin, K. & Freyse, E. J. Wick Technique - Reference Method for Implanted Glucose Sensors. *Artificial Organs* **13**, 453-457 (1989).
- 98 Haaverstad, R., Romslo, I., Larsen, S. & Myhre, H. O. Protein concentration of subcutaneous interstitial fluid in the human leg - A comparison between the wick technique and the blister suction technique. *International Journal of Microcirculation-Clinical and Experimental* **16**, 111-117, doi:10.1159/000179159 (1996).
- 99 Kramer, G. C., Sibley, L., Aukland, K. & Renkin, E. M. Wick Sampling of Interstitial Fluid in Rat Skin - Further Analysis and Modifications of the Method. *Microvascular Research* **32**, 39-49, doi:10.1016/0026-2862(86)90042-7 (1986).
- 100 Heltne, J. K., Husby, P., Koller, M. E. & Lund, T. Sampling of interstitial fluid and measurement of colloid osmotic pressure (COPi) in pigs: evaluation of the wick method. *Laboratory Animals* **32**, 439-445, doi:10.1258/002367798780599848 (1998).
- 101 FDA. *Infusion Pumps*, <<https://www.fda.gov/MedicalDevices/ProductsandMedicalProcedures/GeneralHospitalDevicesandSupplies/InfusionPumps/>> (2016).

- 102 Health, C. *Jackson-Pratt Wound Drains*, <<http://www.cardinalhealth.com/en/product-solutions/medical/infection-control/wound-drains/jackson-pratt-wound-drains.html>> (2017).
- 103 Wientjes, K. J., Vonk, P., Vonk-van Klei, Y., Schoonen, A. J. M. & Kossen, N. W. Microdialysis of glucose in subcutaneous adipose tissue up to 3 weeks in healthy volunteers. *Diabetes Care* **21**, 1481-1488, doi:10.2337/diacare.21.9.1481 (1998).
- 104 Gerritsen, M., Jansen, J. A. & Lutterman, J. A. Performance of subcutaneously implanted glucose sensors for continuous monitoring. *Netherlands Journal of Medicine* **54**, 167-179, doi:10.1016/S0300-2977(99)00006-6 (1999).
- 105 Cirrito, J. R. *et al.* In vivo assessment of brain interstitial fluid with microdialysis reveals plaque-associated changes in amyloid-beta metabolism and half-life. *Journal of Neuroscience* **23**, 8844-8853 (2003).
- 106 Yamada, K. *et al.* In Vivo Microdialysis Reveals Age-Dependent Decrease of Brain Interstitial Fluid Tau Levels in P301S Human Tau Transgenic Mice. *Journal of Neuroscience* **31**, 13110-13117, doi:10.1523/JNEUROSCI.2569-11.2011 (2011).
- 107 Rigby, G. P., Crump, P. & Vadgama, P. Open Flow Microperfusion - Approach to in-Vivo Glucose Monitoring. *Medical & Biological Engineering & Computing* **33**, 231-234, doi:10.1007/BF02523049 (1995).
- 108 Dell'Italia, L. J. *et al.* Compartmentalization of angiotensin II generation in the dog heart - Evidence for independent mechanisms in intravascular and interstitial spaces. *Journal of Clinical Investigation* **100**, 253-258, doi:10.1172/JCI119529 (1997).
- 109 Ellmerer, M. *et al.* in *Proceedings of the 19th Annual International Conference of the Ieee Engineering in Medicine and Biology Society, Vol 19, Pts 1-6: Magnificent Milestones and Emerging Opportunities in Medical Engineering* Vol. 19 *Proceedings of Annual International Conference of the Ieee Engineering in Medicine and Biology Society* 2381-2383 (1997).
- 110 Ellmerer, M. *et al.* Measurement of interstitial albumin in human skeletal muscle and adipose tissue by open-flow microperfusion. *American Journal of Physiology-Endocrinology and Metabolism* **278**, E352-E356 (2000).
- 111 Bodenlenz, M. *et al.* Bioavailability of insulin detemir and human insulin at the level of peripheral interstitial fluid in humans, assessed by open-flow microperfusion. *Diabetes Obesity & Metabolism* **17**, 1166-1172, doi:10.1111/dom.12551 (2015).
- 112 Richer, M. *et al.* Suction-Induced Blister Fluid Penetration of Cefdinir in Healthy-Volunteers Following Ascending Oral Doses. *Antimicrobial Agents and Chemotherapy* **39**, 1082-1086 (1995).
- 113 Eltayib, E. *et al.* Hydrogel-forming microneedle arrays: Potential for use in minimally-invasive lithium monitoring. *European Journal of Pharmaceutics and Biopharmaceutics* **102**, 123-131, doi:10.1016/j.ejpb.2016.03.009 (2016).
- 114 Kitatani, R., Yamada, M., Kamio, M. & Nagai, H. Length Is Associated with Pain: Jellyfish with Painful Sting Have Longer Nematocyst Tubules than Harmless Jellyfish. *Plos One* **10**, doi:10.1371/journal.pone.0135015 (2015).

- 115 Elder, A. & Paterson, C. Sharps injuries in UK health care: a review of injury rates, viral transmission and potential efficacy of safety devices. *Occupational Medicine-Oxford* **56**, 566-574, doi:10.1093/occmed/kql122 (2006).
- 116 Mitsui, T. *et al.* HEPATITIS-C VIRUS-INFECTION IN MEDICAL PERSONNEL AFTER NEEDLESTICK ACCIDENT. *Hepatology* **16**, 1109-1114, doi:10.1016/0270-9139(92)90001-p (1992).
- 117 Pruss-Ustun, A., Rapiti, E. & Hutin, Y. Estimation of the global burden of disease attributable to contaminated sharps injuries among health-care workers. *American Journal of Industrial Medicine* **48**, 482-490, doi:10.1002/ajim.20230 (2005).
- 118 Reaume, S. E. The Use of Hydrofluoric Acid in Making Glass Microneedles. *Science* **116**, 641-641, doi:10.1126/science.116.3023.641 (1952).
- 119 Roberts, D. W. & Granados, R. R. An Inexpensive Device for Pulling Glass Microneedles for Injection of Small Arthropods. *Annals of the Entomological Society of America* **61**, 1042-& (1968).
- 120 Brazzle, J., Papautsky, I. & Frazier, A. B. Micromachined needle arrays for drug delivery or fluid extraction - Design and fabrication aspects of fluid coupled arrays of hollow metallic microneedles. *Ieee Engineering in Medicine and Biology Magazine* **18**, 53-58, doi:10.1109/51.805145 (1999).
- 121 Henry, S., McAllister, D. V., Allen, M. G. & Prausnitz, M. R. Microfabricated microneedles: A novel approach to transdermal drug delivery. *Journal of Pharmaceutical Sciences* **87**, 922-925, doi:10.1021/js980042+ (1998).
- 122 Henry, S., McAllister, D. V., Allen, M. G. & Prausnitz, M. R. Microfabricated microneedles: A novel approach to transdermal drug delivery (vol 87, pg 922, 1998). *Journal of Pharmaceutical Sciences* **88**, 948-948 (1999).
- 123 Lin, L. W. & Pisano, A. P. Silicon-processed microneedles. *Journal of Microelectromechanical Systems* **8**, 78-84, doi:10.1109/84.749406 (1999).
- 124 McAllister, D. V. *et al.* Microfabricated needles for transdermal delivery of macromolecules and nanoparticles: Fabrication methods and transport studies. *Proceedings of the National Academy of Sciences of the United States of America* **100**, 13755-13760, doi:10.1073/pnas.2331316100 (2003).
- 125 Davis, S. P., Martanto, W., Allen, M. G. & Prausnitz, M. R. Hollow metal microneedles for insulin delivery to diabetic rats. *Ieee Transactions on Biomedical Engineering* **52**, 909-915, doi:10.1109/TBME.2005.845240 (2005).
- 126 Gardeniers, H. *et al.* Silicon micromachined hollow microneedles for transdermal liquid transport. *Journal of Microelectromechanical Systems* **12**, 855-862, doi:10.1109/JMEMS.2003.080293 (2003).
- 127 Rajaraman, S. & Henderson, H. T. A unique fabrication approach for microneedles using coherent porous silicon technology. *Sensors and Actuators B-Chemical* **105**, 443-448, doi:10.1016/j.snb.2004.06.035 (2005).
- 128 Verbaan, F. J. *et al.* Assembled microneedle arrays enhance the transport of compounds varying over a large range of molecular weight across human dermatomed skin. *J Control Release* **117**, 238-245, doi:10.1016/j.jconrel.2006.11.009 (2007).

- 129 Verbaan, F. J. *et al.* Improved piercing of microneedle arrays in dermatomed human skin by an impact insertion method. *J Control Release* **128**, 80-88, doi:10.1016/j.jconrel.2008.02.009 (2008).
- 130 Chandrasekaran, S., Brazzle, J. D. & Frazier, A. B. Surface micromachined metallic microneedles. *Journal of Microelectromechanical Systems* **12**, 281-288, doi:10.1109/JMEMS.2003.809951 (2003).
- 131 Griss, P. & Stemme, G. Side-opened out-of-plane microneedles for microfluidic transdermal liquid transfer. *Journal of Microelectromechanical Systems* **12**, 296-301, doi:10.1109/JMEMS.2003.809959 (2003).
- 132 Ji, J., Tay, F. E. H., Miao, J. M. & Iliescu, C. Microfabricated microneedle with porous tip for drug delivery. *Journal of Micromechanics and Microengineering* **16**, 958-964, doi:10.1088/0960-1317/16/5/012 (2006).
- 133 Ma, B. *et al.* A PZT insulin pump integrated with a silicon microneedle array for transdermal drug delivery. *Microfluidics and Nanofluidics* **2**, 417-423, doi:10.1007/s10404-006-0083-x (2006).
- 134 Donnelly, R. F. *et al.* Microneedle-mediated intradermal delivery of 5-aminolevulinic acid: Potential for enhanced topical photodynamic therapy. *J Control Release* **129**, 154-162, doi:10.1016/j.jconrel.2008.05.002 (2008).
- 135 Donnelly, R. F. *et al.* Microneedle Arrays Allow Lower Microbial Penetration Than Hypodermic Needles In Vitro. *Pharmaceutical Research* **26**, 2513-2522, doi:10.1007/s11095-009-9967-2 (2009).
- 136 Haq, M. I. *et al.* Clinical administration of microneedles: skin puncture, pain and sensation. *Biomedical Microdevices* **11**, 35-47, doi:10.1007/s10544-008-9208-1 (2009).
- 137 Gill, H. S., Denson, D. D., Burriss, B. A. & Prausnitz, M. R. Effect of microneedle design on pain in human volunteers. *Clinical Journal of Pain* **24**, 585-594, doi:10.1097/AJP.0b013e31816778f9 (2008).
- 138 Gadkari, R. & Nayak, C. A split-face comparative study to evaluate efficacy of combined subcision and dermaroller against combined subcision and cryoroller in treatment of acne scars. *Journal of Cosmetic Dermatology* **13**, 38-43, doi:10.1111/jocd.12071 (2014).
- 139 Mikszta, J. A. *et al.* Improved genetic immunization via micromechanical disruption of skin-barrier function and targeted epidermal delivery. *Nature Medicine* **8**, 415-419, doi:10.1038/nm0402-415 (2002).
- 140 Davis, S. P., Landis, B. J., Adams, Z. H., Allen, M. G. & Prausnitz, M. R. Insertion of microneedles into skin: measurement and prediction of insertion force and needle fracture force. *Journal of Biomechanics* **37**, 1155-1163, doi:10.1016/j.jbiomech.2003.12.010 (2004).
- 141 Disegi, J. A. & Eschbach, L. Stainless steel in bone surgery. *Injury-International Journal of the Care of the Injured* **31**, S2-S6 (2000).
- 142 Gill, H. S. & Prausnitz, M. R. Coated microneedles for transdermal delivery. *J Control Release* **117**, 227-237, doi:10.1016/j.jconrel.2006.10.017 (2007).

- 143 Yuksel, E. P., Sahin, G., Aydin, F., Senturk, N. & Turanli, A. Y. Evaluation of effects of platelet-rich plasma on human facial skin. *Journal of Cosmetic and Laser Therapy* **16**, 206-208, doi:10.3109/14764172.2014.949274 (2014).
- 144 Dogra, S., Yadav, S. & Sarangal, R. Microneedling for acne scars in Asian skin type: an effective low cost treatment modality. *Journal of Cosmetic Dermatology* **13**, 180-187, doi:10.1111/jocd.12095 (2014).
- 145 Nofal, E., Helmy, A., Nofal, A., Alakad, R. & Nasr, M. Platelet-Rich Plasma Versus CROSS Technique With 100% Trichloroacetic Acid Versus Combined Skin Needling and Platelet Rich Plasma in the Treatment of Atrophic Acne Scars: A Comparative Study. *Dermatologic Surgery* **40**, 864-873, doi:10.1111/dsu.0000000000000091 (2014).
- 146 Badran, M. M., Kuntsche, J. & Fahr, A. Skin penetration enhancement by a microneedle device (Dermaroller (R)) in vitro: Dependency on needle size and applied formulation. *European Journal of Pharmaceutical Sciences* **36**, 511-523, doi:10.1016/j.ejps.2008.12.008 (2009).
- 147 Prausnitz, M. R. Microneedles for transdermal drug delivery. *Advanced Drug Delivery Reviews* **56**, 581-587, doi:10.1016/j.addr.2003.10.023 (2004).
- 148 Cormier, M. *et al.* Transdermal delivery of desmopressin using a coated microneedle array patch system. *J Control Release* **97**, 503-511, doi:10.1016/j.jconrel.2004.04.003 (2004).
- 149 Cui, Q. F., Liu, C. L. & Zha, X. F. Study on a piezoelectric micropump for the controlled drug delivery system. *Microfluidics and Nanofluidics* **3**, 377-390, doi:10.1007/s10404-006-0137-0 (2007).
- 150 Norman, J. J., Brown, M. R., Raviele, N. A., Prausnitz, M. R. & Felner, E. I. Faster pharmacokinetics and increased patient acceptance of intradermal insulin delivery using a single hollow microneedle in children and adolescents with type 1 diabetes. *Pediatric Diabetes* **14**, 459-465, doi:10.1111/pedi.12031 (2013).
- 151 Stevenson, C. L., Santini, J. T. & Langer, R. Reservoir-based drug delivery systems utilizing microtechnology. *Advanced Drug Delivery Reviews* **64**, 1590-1602, doi:10.1016/j.addr.2012.02.005 (2012).
- 152 Wang, P. M., Cornwell, M., Hill, J. & Prausnitz, M. R. Precise microinjection into skin using hollow microneedles. *Journal of Investigative Dermatology* **126**, 1080-1087, doi:10.1038/sj.jid.5700150 (2006).
- 153 Zahn, J. D., Deshmukh, A., Pisano, A. P. & Liepmann, D. Continuous on-chip micropumping for microneedle enhanced drug delivery. *Biomedical Microdevices* **6**, 183-190, doi:10.1023/B:BMMD.0000042047.83433.96 (2004).
- 154 Ito, Y., Yoshimitsu, J. I., Shiroyama, K., Sugioka, N. & Takada, K. Self-dissolving microneedles for the percutaneous absorption of EPO in mice. *Journal of Drug Targeting* **14**, 255-261, doi:10.1080/10611860600785080 (2006).
- 155 Lee, J. W., Park, J. H. & Prausnitz, M. R. Dissolving microneedles for transdermal drug delivery. *Biomaterials* **29**, 2113-2124, doi:10.1016/j.biomaterials.2007.12.048 (2008).

- 156 Sullivan, S. P. *et al.* Dissolving polymer microneedle patches for influenza vaccination. *Nature Medicine* **16**, 915-U116, doi:10.1038/nm.2182 (2010).
- 157 Lee, J. W., Choi, S. O., Felner, E. I. & Prausnitz, M. R. Dissolving Microneedle Patch for Transdermal Delivery of Human Growth Hormone. *Small* **7**, 531-539, doi:10.1002/sml.201001091 (2011).
- 158 Lee, I. C. *et al.* Formulation of two-layer dissolving polymeric microneedle patches for insulin transdermal delivery in diabetic mice. *Journal of Biomedical Materials Research Part A* **105**, 84-93, doi:10.1002/jbm.a.35869 (2017).
- 159 Park, Y. & Kim, B. Skin permeability of compounds loaded within dissolving microneedles dependent on composition of sodium hyaluronate and carboxymethyl cellulose. *Korean Journal of Chemical Engineering* **34**, 133-138, doi:10.1007/s11814-016-0240-1 (2017).
- 160 Qiu, Y. Q. *et al.* Novel lyophilized hydrogel patches for convenient and effective administration of microneedle-mediated insulin delivery. *International Journal of Pharmaceutics* **437**, 51-56, doi:10.1016/j.ijpharm.2012.07.035 (2012).
- 161 Larraneta, E. *et al.* Microwave-Assisted Preparation of Hydrogel-Forming Microneedle Arrays for Transdermal Drug Delivery Applications. *Macromolecular Materials and Engineering* **300**, 586-595, doi:10.1002/mame.201500016 (2015).
- 162 Kearney, M. C., Caffarel-Salvador, E., Fallows, S. J., McCarthy, H. O. & Donnelly, R. F. Microneedle-mediated delivery of donepezil: Potential for improved treatment options in Alzheimer's disease. *European Journal of Pharmaceutics and Biopharmaceutics* **103**, 43-50, doi:10.1016/j.ejpb.2016.03.026 (2016).
- 163 Romanyuk, A. V. *et al.* Collection of Analytes from Microneedle Patches. *Analytical Chemistry* **86**, 10520-10523, doi:10.1021/ac503823p (2014).
- 164 West, D. C., Hampson, I. N., Arnold, F. & Kumar, S. Angiogenesis Induced by Degradation Products of Hyaluronic-Acid. *Science* **228**, 1324-1326, doi:10.1126/science.2408340 (1985).
- 165 Burdick, J. A. & Prestwich, G. D. Hyaluronic Acid Hydrogels for Biomedical Applications. *Advanced Materials* **23**, H41-H56, doi:10.1002/adma.201003963 (2011).
- 166 Tomihata, K. & Ikada, Y. Crosslinking of hyaluronic acid with water-soluble carbodiimide. *Journal of Biomedical Materials Research* **37**, 243-251 (1997).
- 167 Aggarwal, P. & Johnston, C. R. Geometrical effects in mechanical characterizing of microneedle for biomedical applications. *Sensors and Actuators B-Chemical* **102**, 226-234, doi:10.1016/j.snb.2004.04.024 (2004).
- 168 Wang, X., Hagen, J. A. & Papautsky, I. Paper pump for passive and programmable transport. *Biomicrofluidics* **7**, doi:10.1063/1.4790819 (2013).
- 169 Watanabe, T., Hagino, K. & Sato, T. Evaluation of the effect of polymeric microneedle arrays of varying geometries in combination with a high-velocity applicator on skin permeability and irritation. *Biomedical Microdevices* **16**, 591-597, doi:10.1007/s10544-014-9861-5 (2014).

- 170 Donnelly, R. F., Singh, T. R. R. & Woolfson, A. D. Microneedle-based drug delivery systems: Microfabrication, drug delivery, and safety. *Drug Delivery* **17**, 187-207, doi:10.3109/10717541003667798 (2010).
- 171 Castro, C. *et al.* Bacterial cellulose produced by a new acid-resistant strain of *Gluconacetobacter* genus. *Carbohydrate Polymers* **89**, 1033-1037, doi:10.1016/j.carbpol.2012.03.045 (2012).
- 172 Brown, R. M. Cellulose structure and biosynthesis: What is in store for the 21st century? *JOURNAL OF POLYMER SCIENCE PART A-POLYMER CHEMISTRY* **42**, 487-495, doi:10.1002/pola.10877 (2004).
- 173 Klemm, D., Schumann, D., Udhardt, U. & Marsch, S. Bacterial synthesized cellulose - artificial blood vessels for microsurgery. *Progress in Polymer Science* **26**, 1561-1603, doi:Doi 10.1016/S0079-6700(01)00021-1 (2001).
- 174 Sakairi, N. *et al.* Biosynthesis of hetero-polysaccharides by *Acetobacter xylinum* - Synthesis and characterization of metal-ion adsorptive properties of partially carboxymethylated cellulose. *Carbohydrate Polymers* **37**, 409-414, doi:10.1016/S0144-8617(97)00226-9 (1998).
- 175 Cai, J. & Zhang, L. Rapid dissolution of cellulose in LiOH/Urea and NaOH/Urea aqueous solutions. *Macromolecular Bioscience* **5**, 539-548, doi:10.1002/mabi.200400222 (2005).

## Appendix A – Microbial cellulose production and data

### *Culture Protocol*

One of the main biopolymers of interest in this thesis was microbial cellulose. As previously described, microbial (bacterial) cellulose is a specific type of cellulose produced by *G. xylinus* with very interesting properties. Many of these properties, such as high water content and tough nanofibrous network structure, provide potential and even proven advancements in regenerative medicine due to the similarities to native tissues.

Cultivation of bacterial cellulose is not new; in fact, strains of the bacterial family have been passed down from generation to generation as a means to produce vinegar for thousands of years. Although the history of *G. xylinus* is a culinary curiosity, this work required a more systematic and reproducible approach. Thankfully, the culinary history gave a foundation for well established cultivation protocols, which became the bedrock for our cultivation procedure.

High-walled crystalization dishes with lids (Pyrex No. 3250 100x80mm) and modified crystalization dishes with reduced opening diameters to accommodate an inverted petri dish as a lid were used as the initial growth chambers for cellulose pellicles. These chambers were sterilized in an autoclave at before inoculation. Since pellicle production accommodates any shape of a liquid-air boundary, other vessels were experimented with to produce pellicles of various dimensions.

While there are many strains of cellulose-producing bacteria, this work utilized *G. xylinus* (ATCC 700178) for all cellulose production. Cultivation of this bacteria was performed using the standard Hestrin & Schramm Media (HS Media) as preferred in the

literature.<sup>171</sup> HS media was developed by Hestrin & Schramm in 1954 specifically for the production of cellulose.<sup>171-174</sup> The media consists of 20g glucose, 5g yeast extract, 3g Bacto-Peptone, 2.7g dibasic sodium phosphate, and 1.14g citric acid per liter. Due to the volume of production, media was produced in 1L batches. Each batch was neutralized to a pH of 6 before autoclaving.

Dried bacterial samples from ATCC were revived according the protocol. Briefly, for each order, the shipping vial was sanitized in a sterile field, then thermally shattered to release the contents. The inner vial containing the bacteria was filled with 1mL of HS media. 500uL of the resulting bacterial suspension was transferred into two sterile 15mL conical vials containing 5mL HS media and 3 glass beads. The two vials were incubated at 30°C for 3 days before a pulsed vortex, used to distribute the revived bacteria throughout the inoculation media.

Fifteen of the aforementioned sterilized culture vessels were filled with 45mL of fresh, sterile HS media. To each of these was added 2mL of the inoculation media. The inoculated vessels were then incubated under static atmospheric conditions at 30°C for two weeks to develop a base pellicle. Because the base pellicle does not form as uniformly as subsequent layers, it is used as the inoculation pellicle for later batches.

Every week after the base pellicle was formed, 50mL of fresh HS media was added to each culture vessel. Because pellicles form at the liquid-air interface, a new pellicle would form at each layer each week until the vessel was filled. Filling of the vessels required 5 weeks

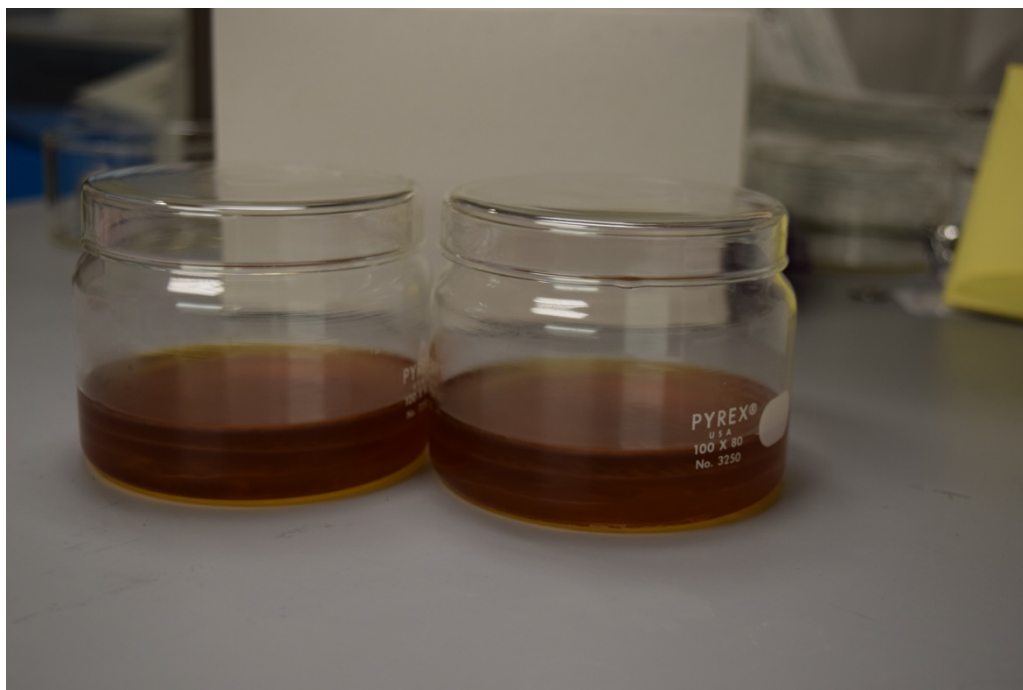


**Figure A1:** Growth of cellulose pellicles. Clear layering is seen between the cellulose and media where cellulose grows at the liquid air interface.

after the formation of the base layer. **Figure A1** depicts a culture dish of cellulose before harvest. Current protocol yields approximately 75 pellicles every five weeks.

Harvesting the cellulose was a straightforward process. Because the pellicles grew in separate layers, removal of the layers using forceps was very simple. The top layers were separated into a 4L beaker and the base layers were allowed to remain in their respective dish in order to inoculate the following batch. Because the base layer was already established, the 50mL HS media feedings could begin immediately without the 2 week growth period.

There are many procedures for purification of cellulose pellicles depending on the desired application of the final product. Initially, the pellicles were soaked in tap water for 24 hours with water exchanges every 8 hours. Once the bulk of the media was removed, the

cellulose was transferred to a 1M KOH bath to sterilize the pellicle and dissolve the bacteria inside. KOH was used over other bases because the sodium and lithium ions have been shown to weaken the cellulose crystal structure.<sup>175</sup> Since the high crystallinity of bacterial cellulose was a property of interest, every option to maintain that structure was utilized.

Following a 24-48 hour soak in KOH, the cellulose was transferred to a 0.5M HCl bath to neutralize the base. After a 1 hour neutralization, the cellulose was rinsed repeatedly in DI water 4 hours each rinse until colorless. Finally, the cellulose was stored in fresh DI water, which was converted into a 0.1mM sodium azide solution in order to prevent contamination. Multiple mass difference calculations provided evidence that a hydrated BC pellicle was 99% water by mass.

### *Mechanical Testing*

Never dried cellulose pellicles were cut into “dog-bones” using a laser cutter. Each 4” sheet produced 6 dog-bones. In order to test the mechanical strength of cellulose, these dog-bones were then either dried to get data for cellulose controls or soaked in a photopolymerizable PEG solution for 24h before polymerizing. The dogbones were dried on a silicon mat at ambient conditions, then placed on an INSTRON mechanical testing device.

As described previously, microbial cellulose has some unique mechanical properties, which are determined by how wet it’s sheets are and if they have been previously dried. In the mechanical testing experiments, never dried, dried and rewetted, and dry cellulose dogbones were analyzed to determine the interactions between cellulose and interpenetrating polymer networks.

Because cellulose has a smooth surface, sandpaper was attached to the grips of the INSTRON prior to experimentation. When ready, the cellulose dogbones were placed into the grips, spaced 25mm apart, such that the wide ends were clamped while the narrow middle was not. This was done to ensure the stress was concentrated uniformly in the middle of the dogbone. The dogbone was then pulled at 3mm/min until break. The break-point was often very identifiable, but it is important to note that even with the sandpaper, some slippage of the material was often observed and could contribute to variations in Young's Modulus if included in the data. Samples with clear indication of slippage were excluded from the provided data.

## ***Results & Discussion***

### ***Mechanical Properties***

The mechanical properties of cellulose as a reinforcing agent were evaluated using an INSTRON mechanical analyzer. Based on the data, cellulose composite materials act as a reinforcing scaffold for otherwise weak materials. In **Figure A2**, cellulose max stress at break (indicated by the blue line) is improved when used in addition to PEG. PEG is inherently a mechanically weak material, but the formation of the composite significantly improved the ability of cellulose and PEG to hold stress.

**Figure A3** shows the max strain at break. Strain in the cellulose/PEG composites is relatively like that of cellulose, showing that cellulose dominates the mechanical resistance to

### PEG-TE/PEG-NB Max Stress: Dry

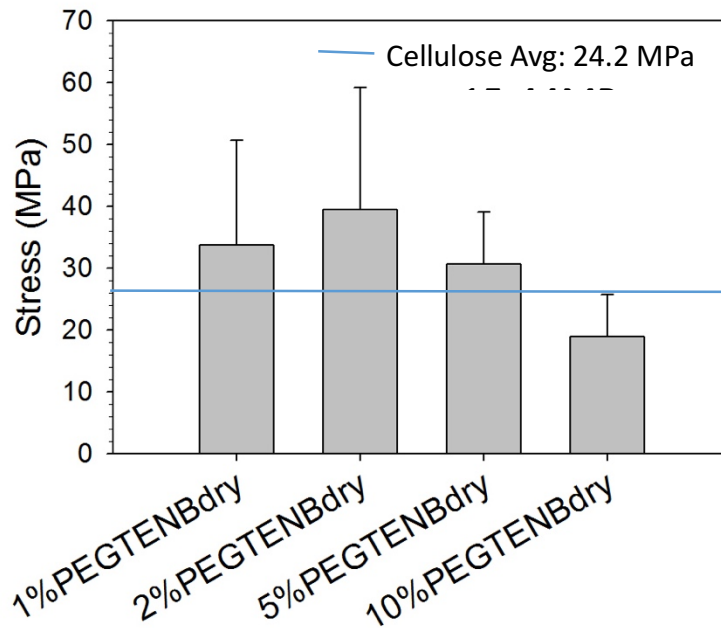


**Figure A2:** Mechanical stress endured by cellulose/PEG-based interpenetrating networks.

deformation. Similar to the stress test, the higher PEG concentration breaks the trend and shows higher strain at break. Pairing these two sets of data, it can be concluded that cellulose dominates the mechanical properties of a composite material to a certain point.

Because PEG is too weak of a material by itself, it is difficult to obtain a direct correlation by varying the compositions of the polymers. When comparing this data to what was observed in the compression data for the HA based microneedles however, it is reasonable to assume that cellulose is indeed a reinforcing material, even at low concentrations.

### PEG-TE/PEG-NB Strain at Break: Dr

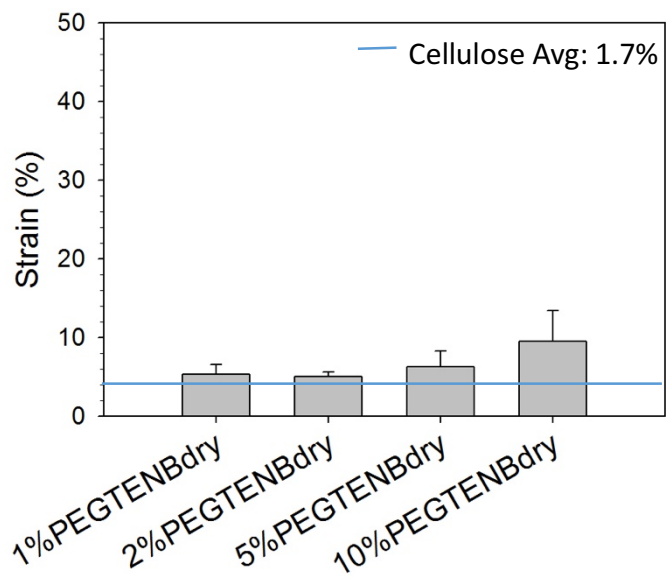


**Figure A3:** Mechanical strain endured by cellulose/PEG-based interpenetrating networks.